AD NUMBER
AD015178
CLASSIFICATION CHANGES
TO: **unclassified**
FROM: **confidential**
LIMITATION CHANGES
TO: **Approved for public release; distribution is unlimited.**
FROM: **Distribution authorized to U.S. Gov't. agencies and their contractors; Administrative/Operational Use; 03 JUN 1952. Other requests shall be referred to Naval Ordnance Lab., White Oak, MD.**
AUTHORITY
30 Jun 1965, DoDD 5200.10; NOL ltr, 29 Aug 1974

CONFIDENTIAL

NAVORD REPORT 2687

WIND TUNNEL INVESTIGATION OF THE RS-9 METEOR AT MACH NUMBER 2.87

3 June 1952

U. S. NAVAL ORDNANCE LABORATORY

WHITE OAK, MARYLAND

CONFIDENTIAL

SECURITY INFORMATION

CONFIDENTIAL
NAVORD Report 2687

Aeroballistic Research Report 77

WIND TUNNEL INVESTIGATION OF THE RS-9 METEOR AT MACH NUMBER 2.87

Prepared by:

T. M. Clancy

ABSTRACT: The results of an investigation in the 40 x 40 cm Aeroballistics Tunnel Number 1 to determine pitch, yaw, and rolling moment data for the RS-9 Meteor are presented in this report. The data were obtained at Mach number 2.87.

U. S. NAVAL ORDNANCE LABORATORY
WHITE OAK, MARYLAND

SECURITY INFORMATION

NAVORD Report 2687 3 June 1952

This investigation was performed at the request of the Massachusetts Institute of Technology, reference (a). The wind-tunnel data were obtained 14 through 17 November 1951 inclusive. The investigation was performed under task NOL-Rexa-1-52.

The purpose of this investigation was to obtain pitch, yaw, and rolling moment data at Mach number 2.87 which are needed for an analysis of the stability and control characteristics of the RS-9 Meteor.

This document may include technical data or other information which may be proprietary to parties other than the government and therefore the transmission by the Department of the Navy of this document is not to be regarded by implication or otherwise, as licensing or conveying any rights or permission to the recipient or any other person or corporation gaining access to this document to use for commercial purposes, as distinguished from governmental purposes, the said technical data or information disclosed herein.

E. L. WOODYARD
Captain, USN
Commander

H. H. KURZWEG, Chief
Aeroballistic Research Department
By direction

CONTENTS

ILLUSTRATIONS

WIND-TUNNEL INVESTIGATION OF THE RS-9 METEOR AT MACH NUMBER 2.87

INTRODUCTION

1. The RS-9 Meteor is an air-to-air missile being designed by the Massachusetts Institute of Technology for the Bureau of Ordnance. The missile is of the interdigitated canard-wing type designed to operate in a Mach number range from 1.25 to 3.00. Previous investigations have been conducted on the RS-9 configuration in the NOL 40 x 40 cm Aeroballistics Tunnel Number 1 at Mach number 1.57 (Reference b), and in the MIT tunnel at Mach numbers 2.0 and 2.5.

2. In order to determine more completely the stability and control characteristics of the Meteor for its range of design Mach numbers, a 1/9th scale model was tested in the NOL 40 x 40 Aeroballistics Tunnel Number 1. Five component force data comprising pitch, yaw, and roll were obtained in this test at Mach number 2.87. Control effectiveness characteristics of the RS-9 missile were determined with the control surfaces of the horizontal and vertical canards fixed at 8°, 16°, and 24°. The rollerons on the wings had fixed deflections of 8°, 16°, and 24°.

SYMBOLS

- A = maximum cross-sectional area (0.660 sq. in.)
- C_Z = normal force coefficient = $\frac{F_Z}{qA}$
- C_θ = pitching moment coefficient (referred to the center of gravity of the missile: 47.4% ℓ from base, or 6.323 in. from base of model) = $\frac{M_\theta}{qAd}$
- C_Y = lateral force coefficient = $\frac{F_Y}{qA}$
- C_ψ = yawing moment coefficient (referred to center of gravity) = $\frac{M_\psi}{qAd}$
- C_ϕ = rolling moment coefficient = $\frac{M_\phi}{qAd}$
- C_{ϕ_c} = rolling moment coefficient corrected for pitch and yaw interactions
- d = maximum body diameter (0.917 in.)
- ℓ = model length (13.333 in.)
- M = Mach number (2.87)
- q = dynamic pressure (2.78 psi)
- R = Reynolds number based on model length in feet (2.89×10^6)
- α = angle of attack
- ψ = angle of yaw
- ϕ = roll angle of model on balance

MISSILE NOTATION

B	Body-alone
W	Wings with antennae on two surfaces (see Figure 1)
W^o	Wings with no antennae
C_H	Horizontal Canards with control surfaces at 0° deflection
C_V	Vertical Canards with control surfaces at 0° deflection
C_{H_x}	Horizontal Canards with control surfaces at x° deflection

Positive pitching moment is designated as an overturning moment when the missile is at a positive angle of attack. The sign convention for yaw is similar to that for pitch.

Positive roll is designated as clockwise when looking forward from the base of the missile.

DESCRIPTION OF THE MODEL AND BALANCE

3. A sketch of the full-scale missile configuration is shown in Figure 1. A 1/9th scale model designed and constructed by missile project personnel at MIT was used for the tunnel tests. In all runs except run 41, the model was oriented in the wind tunnel so that a pair of canards was located in the plane of yaw (as shown in Figure 1). In run 41 the model was rolled -45°, to the orientation shown in Figure 1.

4. Control surfaces on the horizontal and vertical canards were deflected so as to produce positive forces in the pitch and yaw planes respectively. The rollerons, differentially deflected, were set to produce negative rolling moment.

5. The internal, five component strain gage balance used to measure normal and lateral forces, pitch, yaw, and rolling moments was designed and constructed at MIT. A yaw device was incorporated into the design of the sting in the form of a sliding cartridge at the base of the sting that was adjustable from -15° to 15° yaw.

DATA REDUCTION AND CORRECTIONS

7. Corrections to the angle of attack were computed from the following formula:

$$\Delta \alpha = AC_Z + BC_\theta$$

Similarly, yaw angles were corrected using the formula:

$$\Delta \psi = EC_y + FC_\psi$$

The constants A, B, E, and F were determined by statically loading the model in pitch and yaw at several locations.

8. The pitch and yaw gages were alined to normal planes by electrical shunting. The effects of pitch and yaw forces on the roll gage were substantially reduced by this method; the remaining interactions, however, were removed by the following formula:

$$C_{\phi_C} = C_\phi + T_1 C_n + T_2 C_e + T_3 C_y + T_4 C_\psi$$

where:

T_1 = correction due to normal force (-.000694)

T_2 = correction due to pitching moment (-.001005)

T_3 = correction due to lateral force (+.000917)

T_4 = correction due to yawing moment (-.000612)

The interaction constants, T_1, T_2, T_3, and T_4 were obtained from static calibration of the balance. It can be seen from the values given above that the corrections to the roll moment coefficient were very small.

9. The accuracy of the recording instruments was ± 2.4 helipot divisions (ohms) in a range from 0 to 500 divisions, corresponding to an error in the coefficients of the order of ± 1%.

RESULTS

10. The data are plotted in coefficient form versus angle of attack in Figures 2 through 37.

11. The values of angle of attack used for the plotted data are the indicated sector angles corrected for sting deflection. In plotting angles of yaw, however, only the angles indicated on the yaw device were used. The corrected yaw angles are given in Table I.

12. The pitching moment curve for the body-wing configuration in zero roll attitude (Figure 6) is linear to approximately 4° angle of attack. At higher angles, however, there is a decrease in wing effectiveness. The same configuration rolled -45° (so that the wing antennae are in the plane of yaw) produces a more stable pitch curve with no noticeable decrease in wing effectiveness up to 18°. The non-linearity of the former pitch curve can then most probably be attributed to the non-symmetrical disposition of the antennae on the wings.

13. The magnitude of the roll data for runs 9 through 42 and run 44 is not compatible with data taken more recently, and should be used with discretion.

14. At Mach 2.87 the standard Meteor configuration is neutrally stable at small angles, becoming unstable at approximately 14° angle of attack, Run 7, Figure 8. A comparison of runs 7 and 40 reveals that the wing antennae have a negligible effect on the stability. This is to be expected because the wings themselves are comparatively ineffective. The canard antennae*, on the other hand, while contributing very little (5% at most) to the total normal force of the missile, have a decidedly destabilizing effect for the following reasons:

(1) the forces on the canard antennae act through greater distances to the center of gravity of the missile.

(2) the canards and their antennae are efficient lifting surfaces.

15. The most important reason however, especially with regard to the lower angles of attack is that the addition of antennae to the canards results in stronger tip vortices that create a downwash on the wings and decrease their effectiveness.

16. Tests of the RS-9 configuration at Mach 1.57 show that there is a sharp increase in stability occurring between 9 and 10° angle of attack, reference (b). This break in the pitch curve corresponds to the point at which the vortices from the horizontal canard tips cross over the upper wing surfaces. The same tendency is evidenced (but to a lesser extent) at higher Mach numbers. It is very probable that removal of the antennae from the canards will result in a more stable, and nearly linear pitching moment curve.

* Since the standard missile orientation in the wind tunnel places a pair of canards in the plane of yaw, it is these horizontal antennae to which the following discussion relates.

REFERENCES

(a) Alden, H. T. - Aeroballistic Research Request (ARR 192) (Conf) (1951)

(b) Clancy, T. M. - Aeroballistic Research Investigation of the RS-9 Meteor (Conf) (1951)

TABLE I

List of Runs

Run	Conf.	ψ corr	ϕ	Figure Pitch	Figure Yaw & Roll	Remarks
1	B	0	0	3	4	
2	BC_HC_v	0	0	3	4	
3	$BC_{H8}C_v$	0	0	5	6	
4	$BC_{H16}C_v$	0	0	5	6	
5	$BC_{H24}C_v$	0	0	5	6	
6	BW	0	0	7	8	
7	BWC_HC_v	0	0	9,23,37	10,24,38	
8	BWC_HC_v	0	180°	37	38	Model Rolled 180° Balance Upright
9	$BWC_{H8}C_v$	0	0	11	12	
10	$BWC_{H16}C_v$	0	0	11	12	
11	$BWC_{H24}C_v$	0	0	11	12	
12	BWC_HC_{v16}	0.05	0	23	24	
13	BWC_HC_{v16}	5.18	0	25	26	
14	BWC_HC_v	5.12	0	25	26	
15	$BWC_{H8}C_v$	5.12	0	13	14	
16	$BWC_{H16}C_v$	5.12	0	13	14	
17	$BWC_{H24}C_v$	5.12	0	13	14	
18	BWC_HC_v	10.27	0	27	28	
19	$BWC_{H8}C_v$	10.26	0	15	16	

TABLE I (continued)

List of Runs

Run	Conf.	ψ corr	ϕ	Figure		Remarks
				Pitch	Yaw & Roll	
20	$BWC_{H16}C_v$	10.26	0	15	16	
21	$BWC_{H24}C_v$	10.26	0	15	16	
22	$BWC_{H24}C_{v16}$	10.33	0	29	30	
23	BWC_HC_{v16}	10.33	0	27,29	28,30	
24	BWC_HC_{v16}	15.53	0	31	32	
25	BWC_HC_v	15.45	0	31	32	
26	$BWC_{H8}C_v$	15.45	0	17	18	
27	$BWC_{H16}C_v$	15.45	0	17	18	
28	$BWC_{H24}C_v$	15.43	0	17	18	
29	BW	15.18	0	19	20	
30	$BW_8C_HC_v$	15.44	0	35	36	
31	$BW_{16}C_HC_v$	15.45	0	35	36	
32	$BW_{24}C_HC_v$	15.44	0	35	36	
33	BC_HC_v	15.49	0	19	20	
34	$BC_{H8}C_v$	15.48	0	21	22	
35	$BC_{H16}C_v$	15.48	0	21	22	
36	$BC_{H24}C_v$	15.48	0	21	22	
37	$BW_8C_HC_v$	0	0	33	34	
38	$BW_{16}C_HC_v$	0	0	33	34	

TABLE I (continued)

List of Runs

Run	Conf.	ψ corr	ϕ	Figure Pitch	Figure Yaw & Roll	Remarks
39	$BW_{24}C_HC_v$	0	0	33	34	
40	$BW^{8}C_HC_v$	0	0	9	10	
41	BW	0	-45°	7	8	
42	BWC_HC_v	0	0	37	38	Balance Rotated 180°
43	$BWC_{H8}C_v$	0	0	--	--	Repeat Run(not plotted)
44	BWC_HC_{v16}	5.17	0	--	--	Repeat Run(not Plotted)

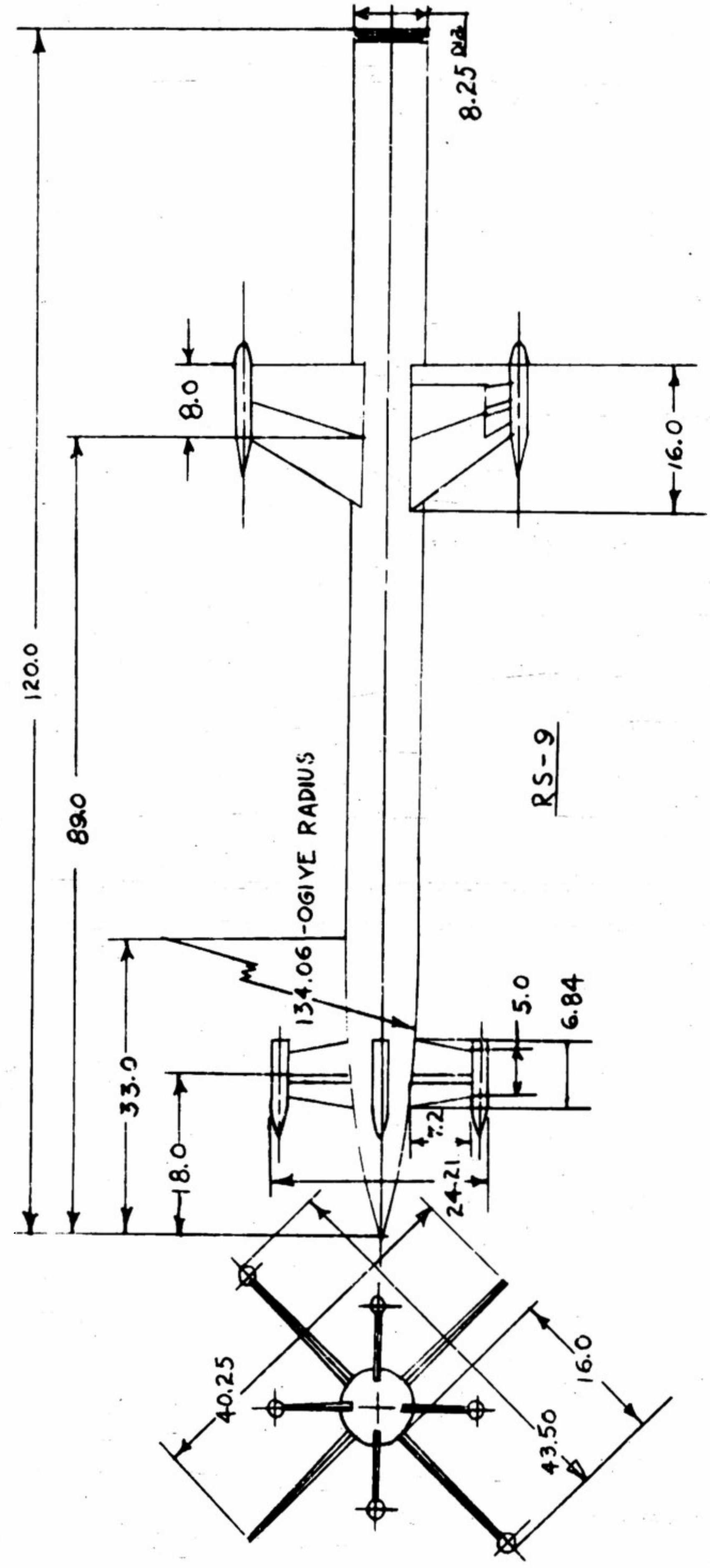

SUPERSONIC TUNNEL MODEL ~1/9 SCALE
DIMENSIONS SHOWN-FULL SCALE
ALL DIMENSIONS IN INCHES

FIGURE I

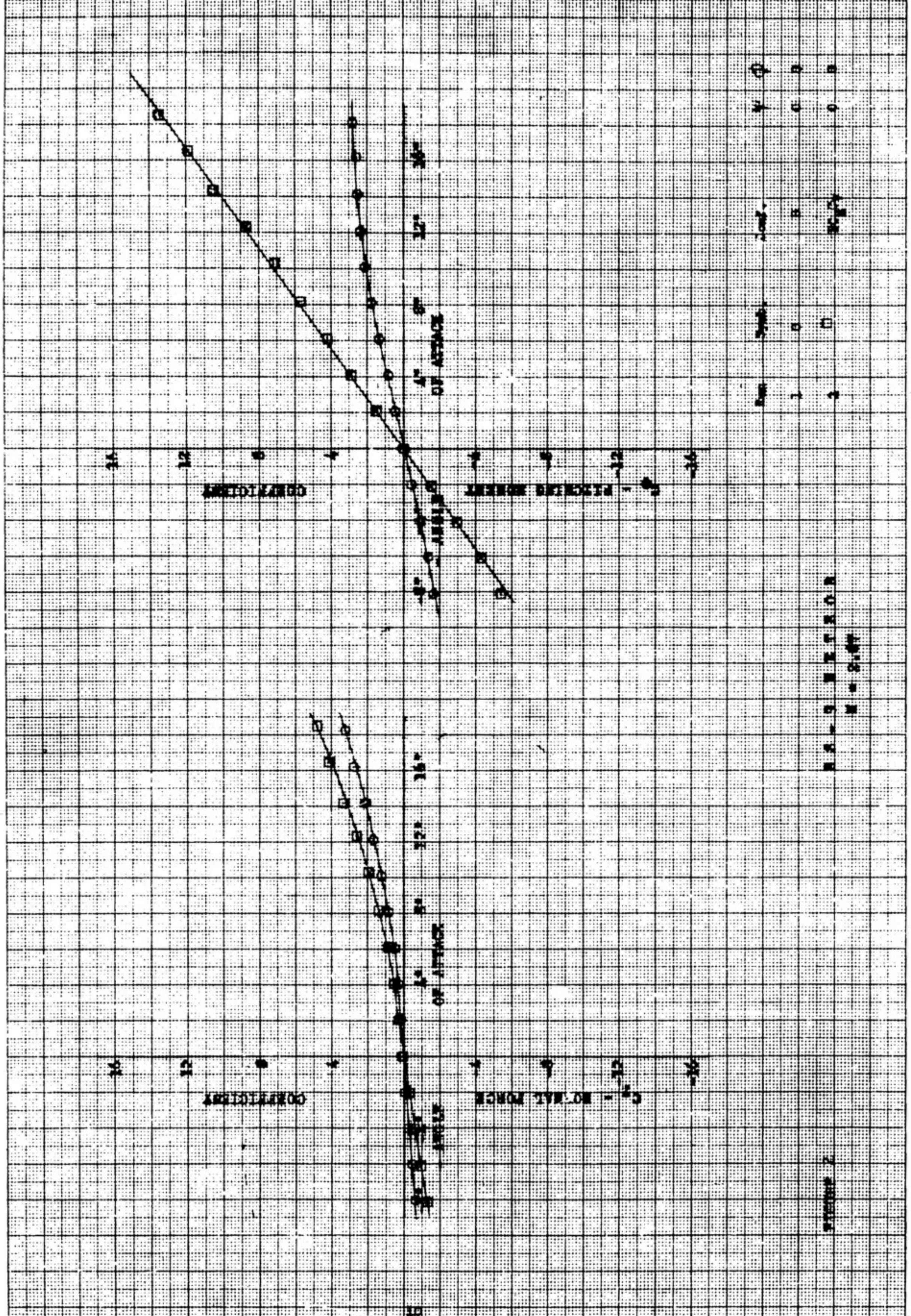

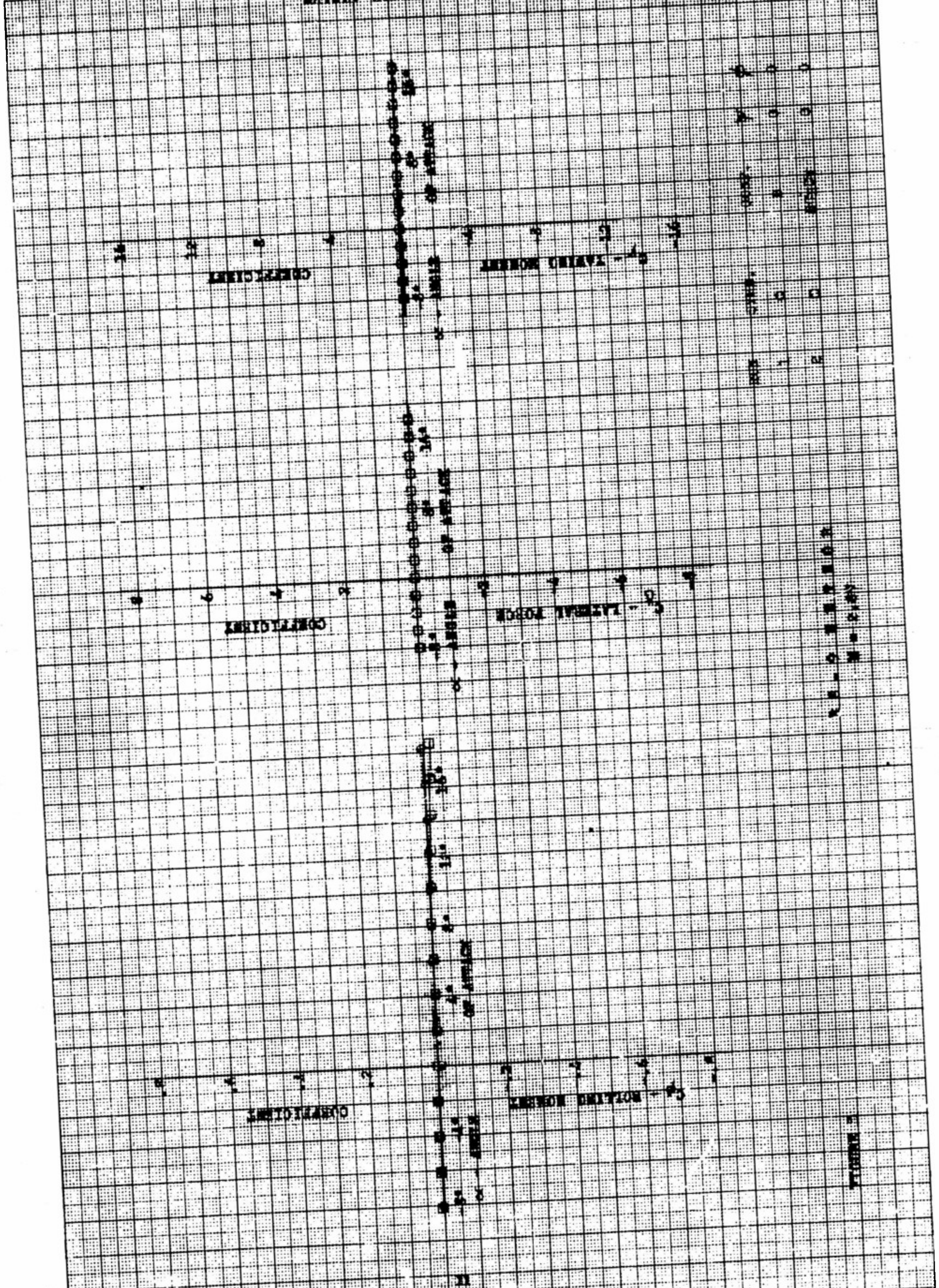

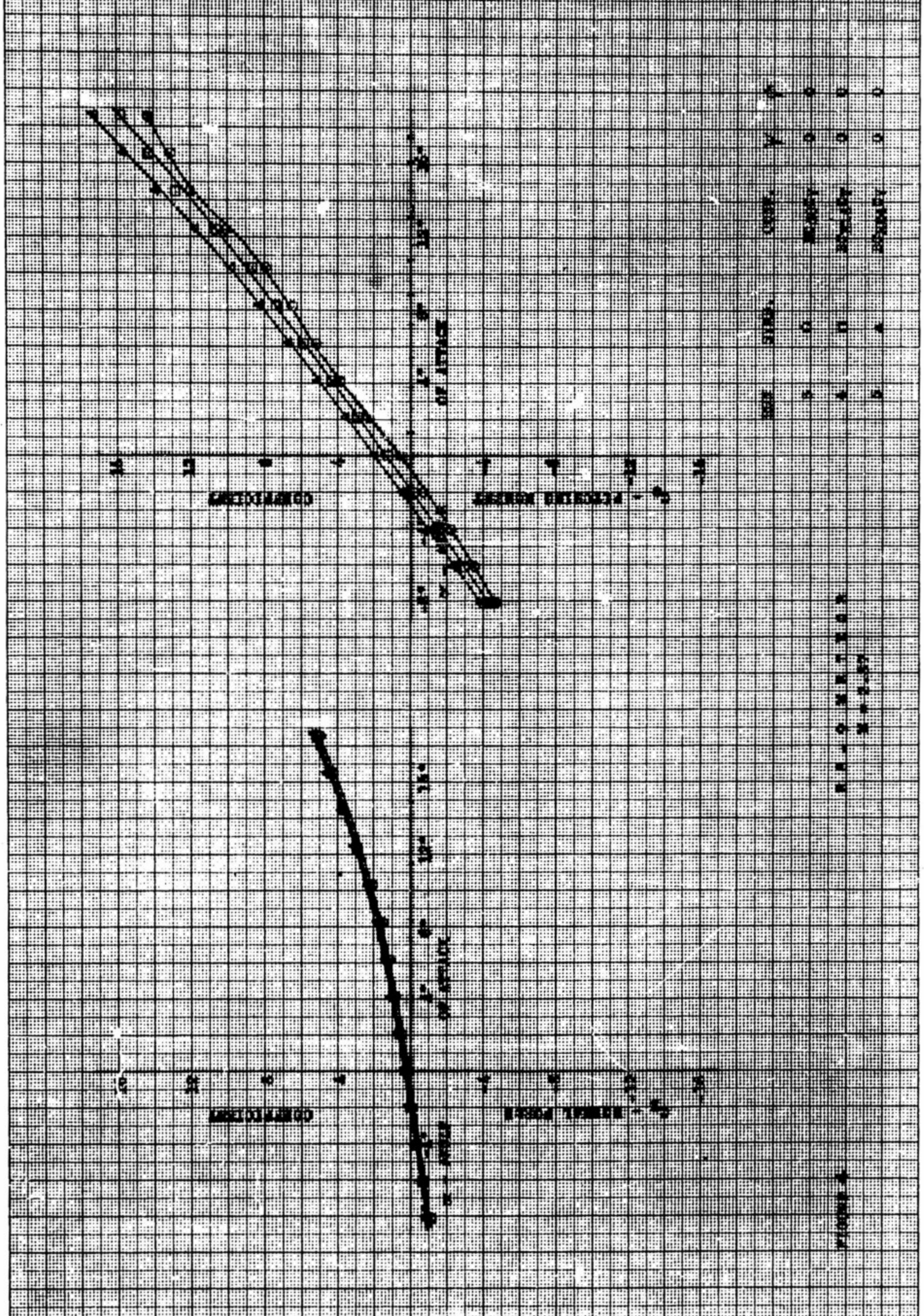

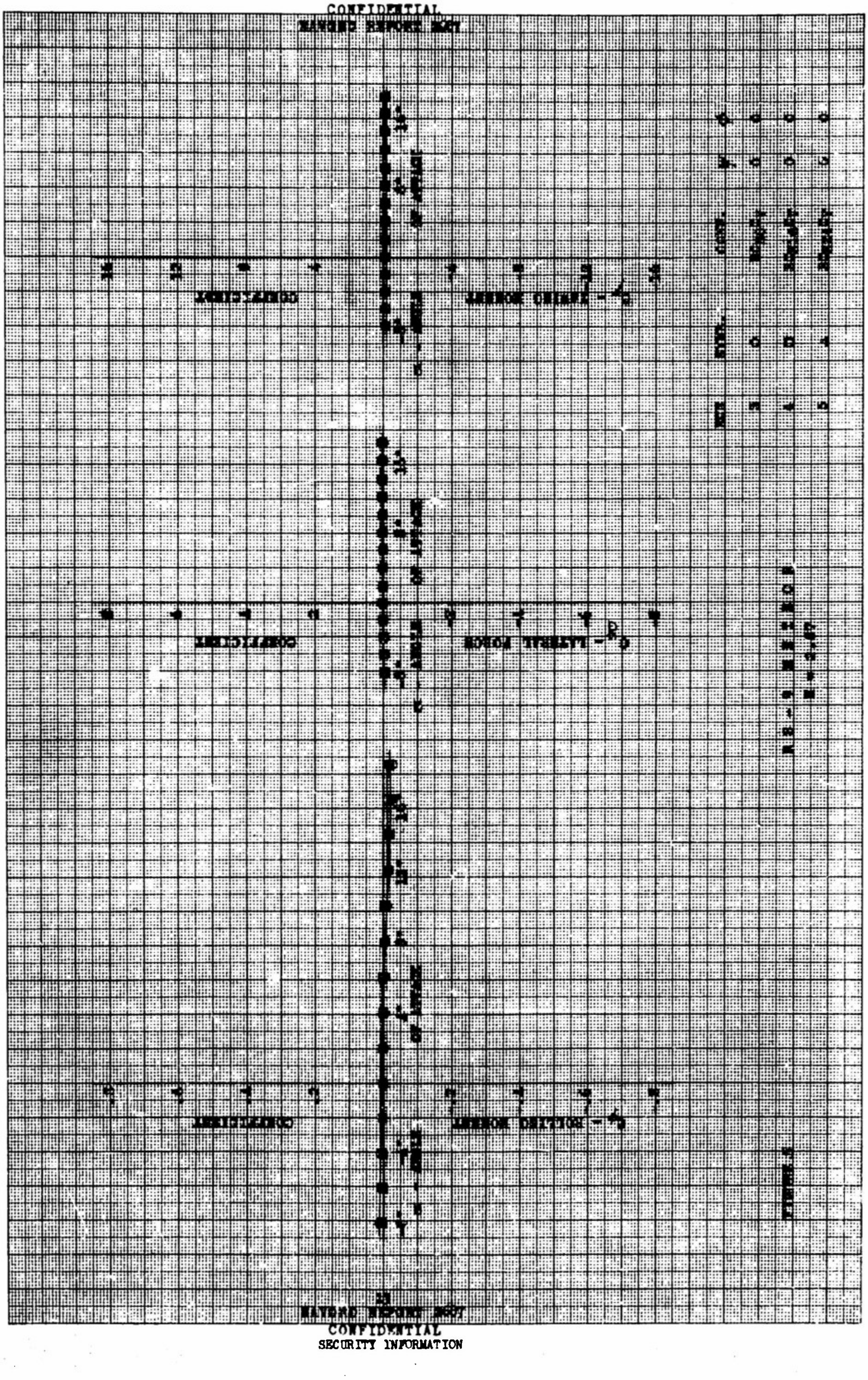

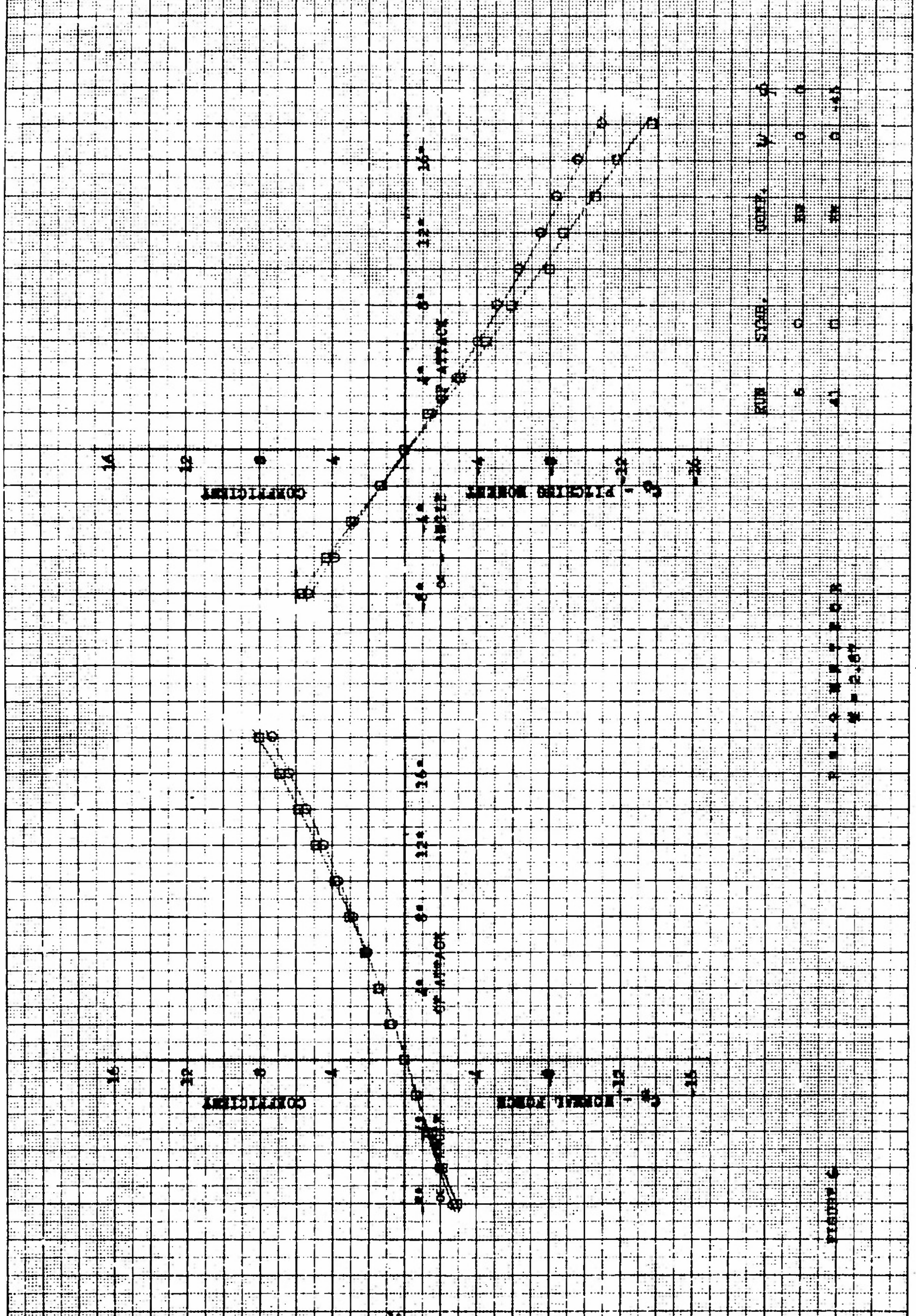
PITCHING MOMENT COEFFICIENT
NORMAL FORCE COEFFICIENT
ANGLE OF ATTACK
RUN
SYMB.
FIGURE 6

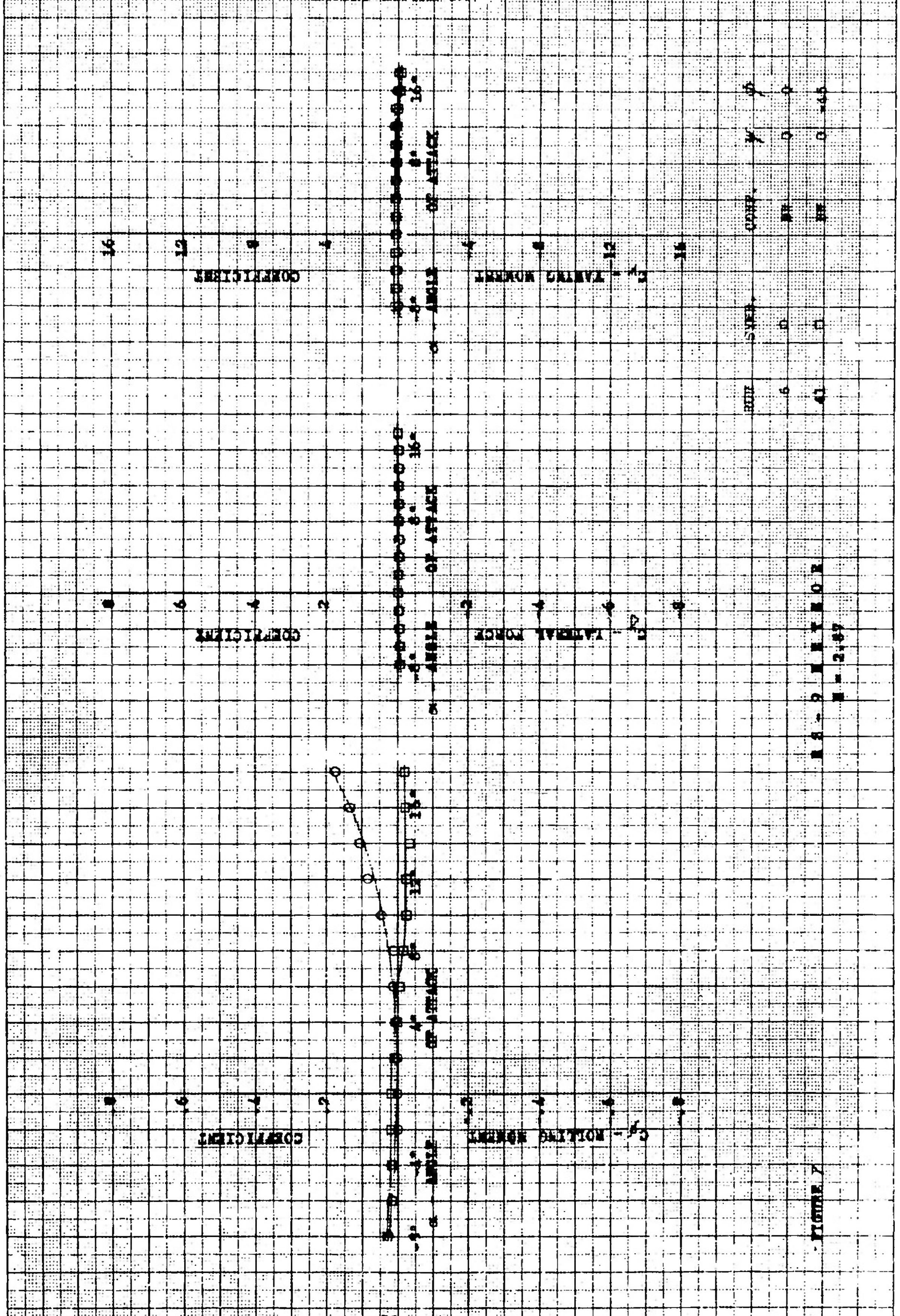
YAWING MOMENT COEFFICIENT
LATERAL FORCE COEFFICIENT
ROLLING MOMENT COEFFICIENT
ANGLE OF ATTACK
RUN
SYMB.
CONF.

FIGURE 7

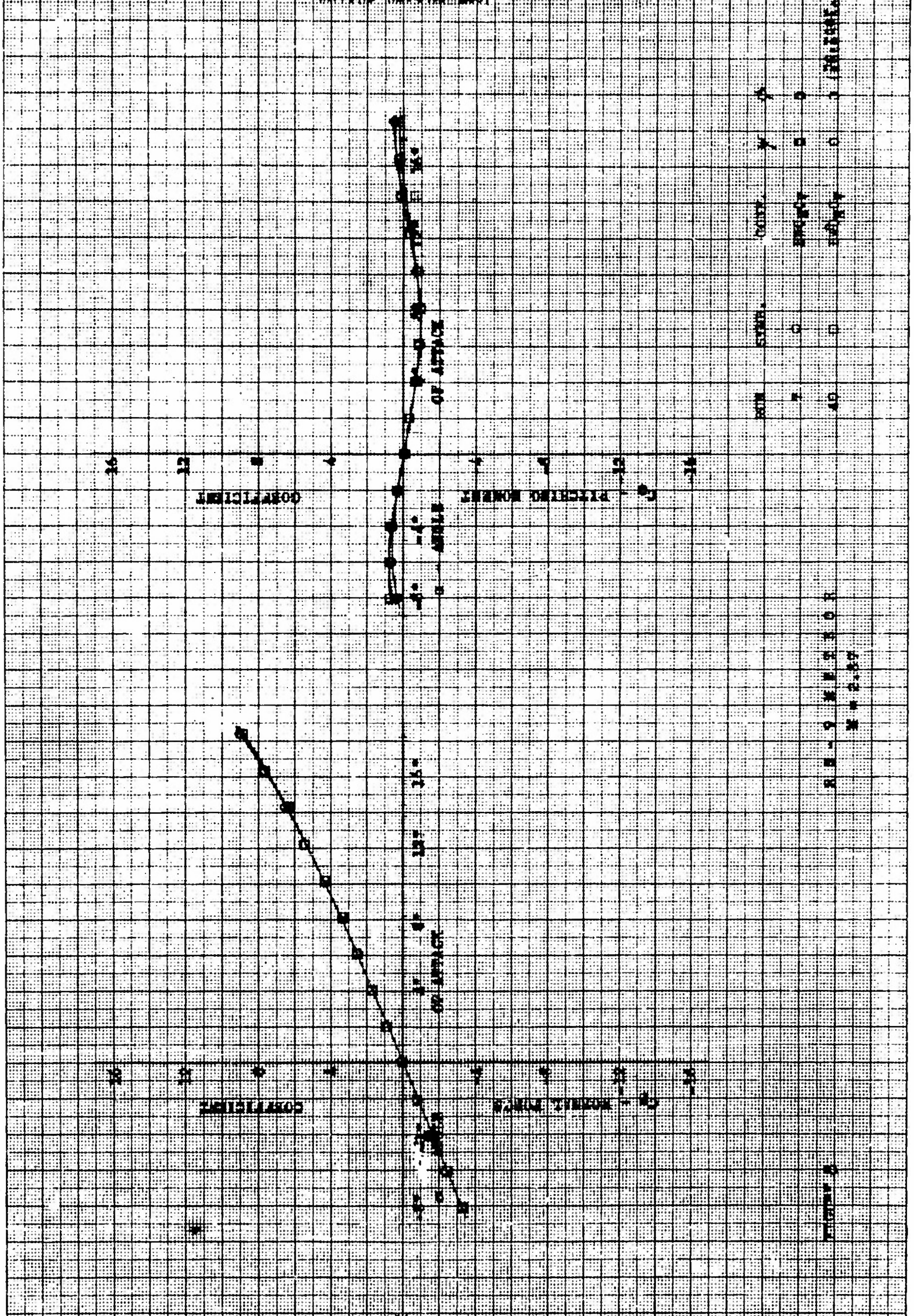
COEFFICIENT
NORMAL FORCE
PITCHING MOMENT
ANGLE
OF ATTACK
RUN
SYMB.
CONF.

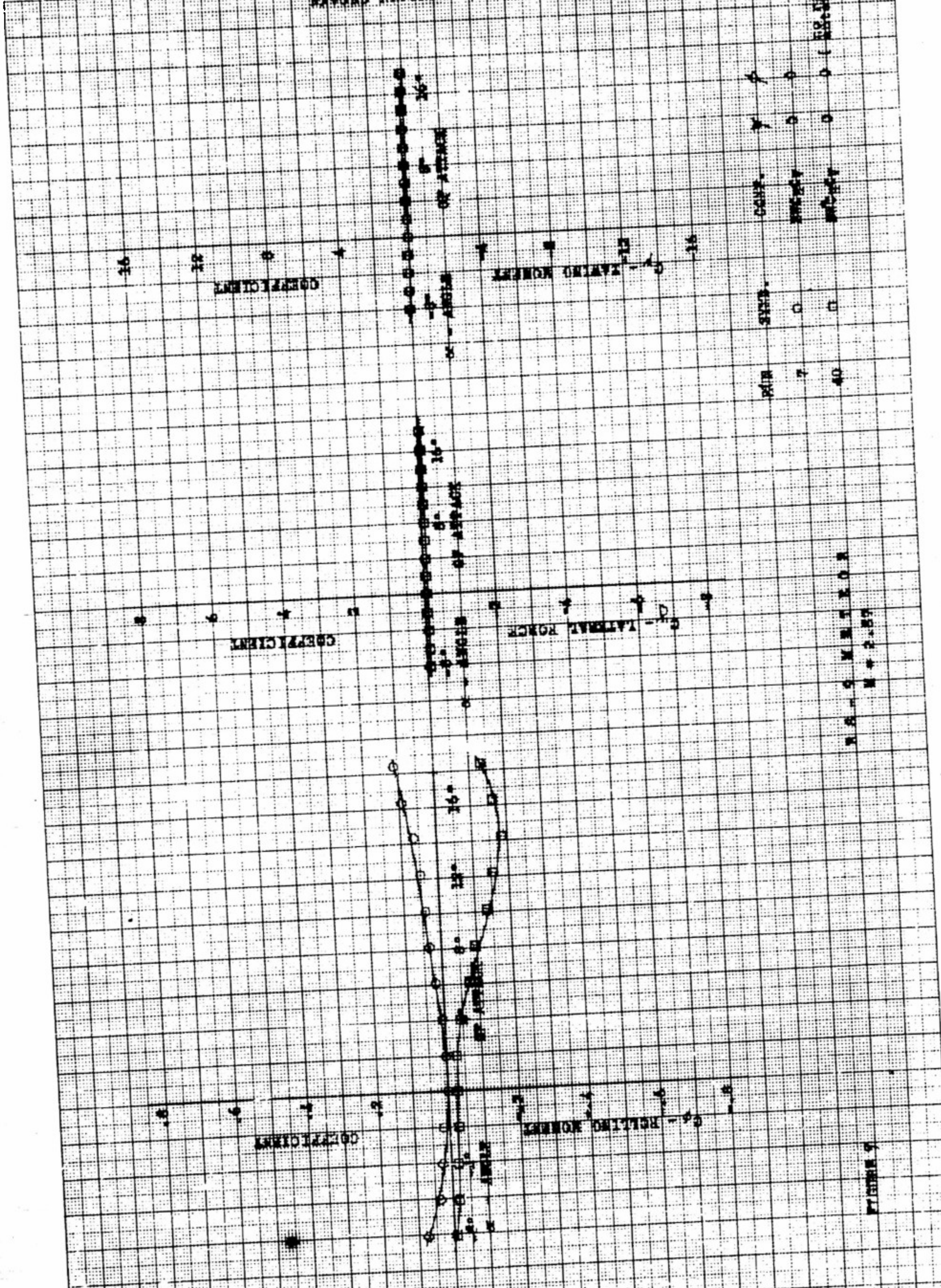

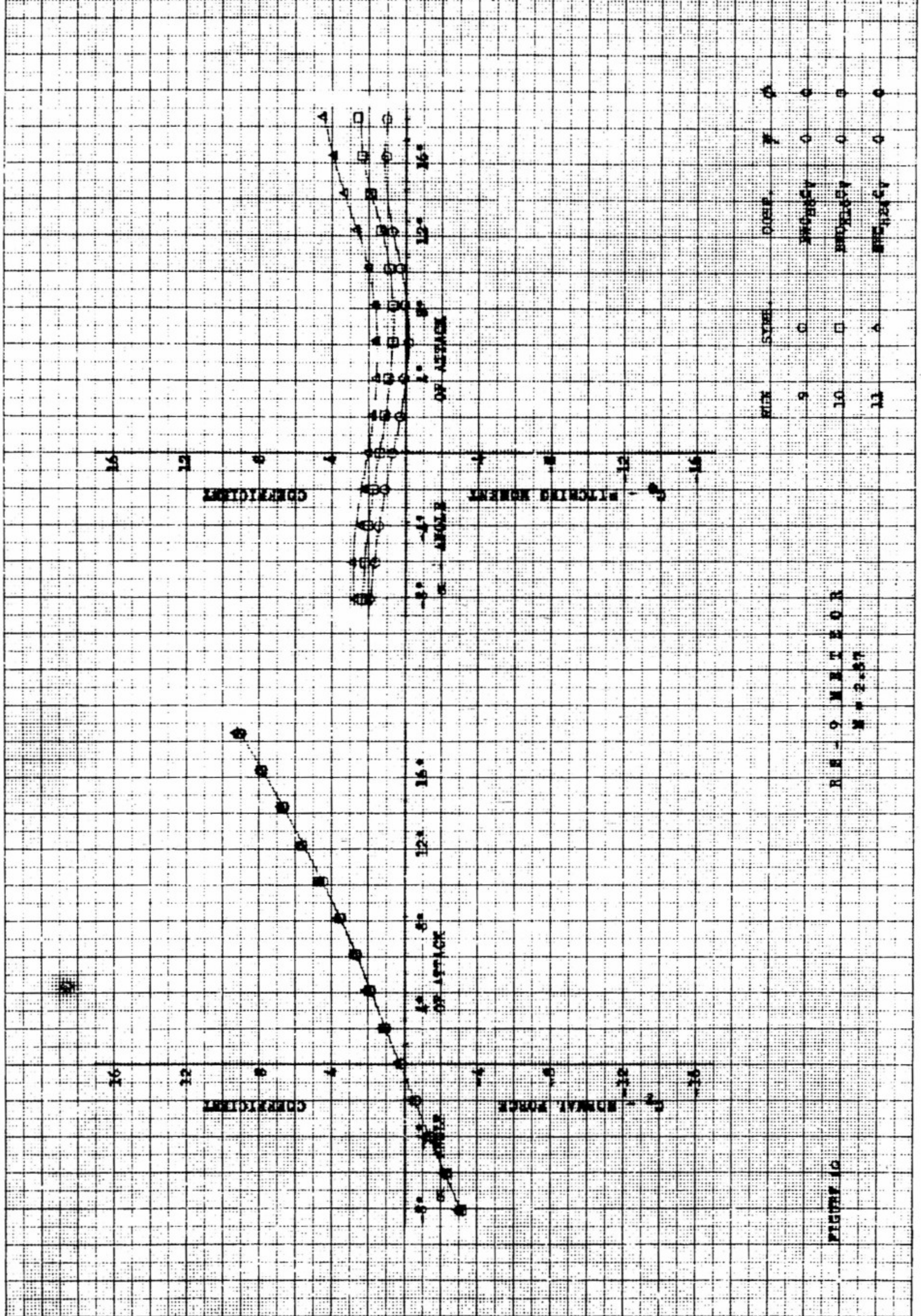
C_m - PITCHING MOMENT COEFFICIENT
α - ANGLE OF ATTACK
C_N - NORMAL FORCE COEFFICIENT
RUN
SYMB.
9
10
11
RS-9 METEOR
M = 2.57

FIGURE 10

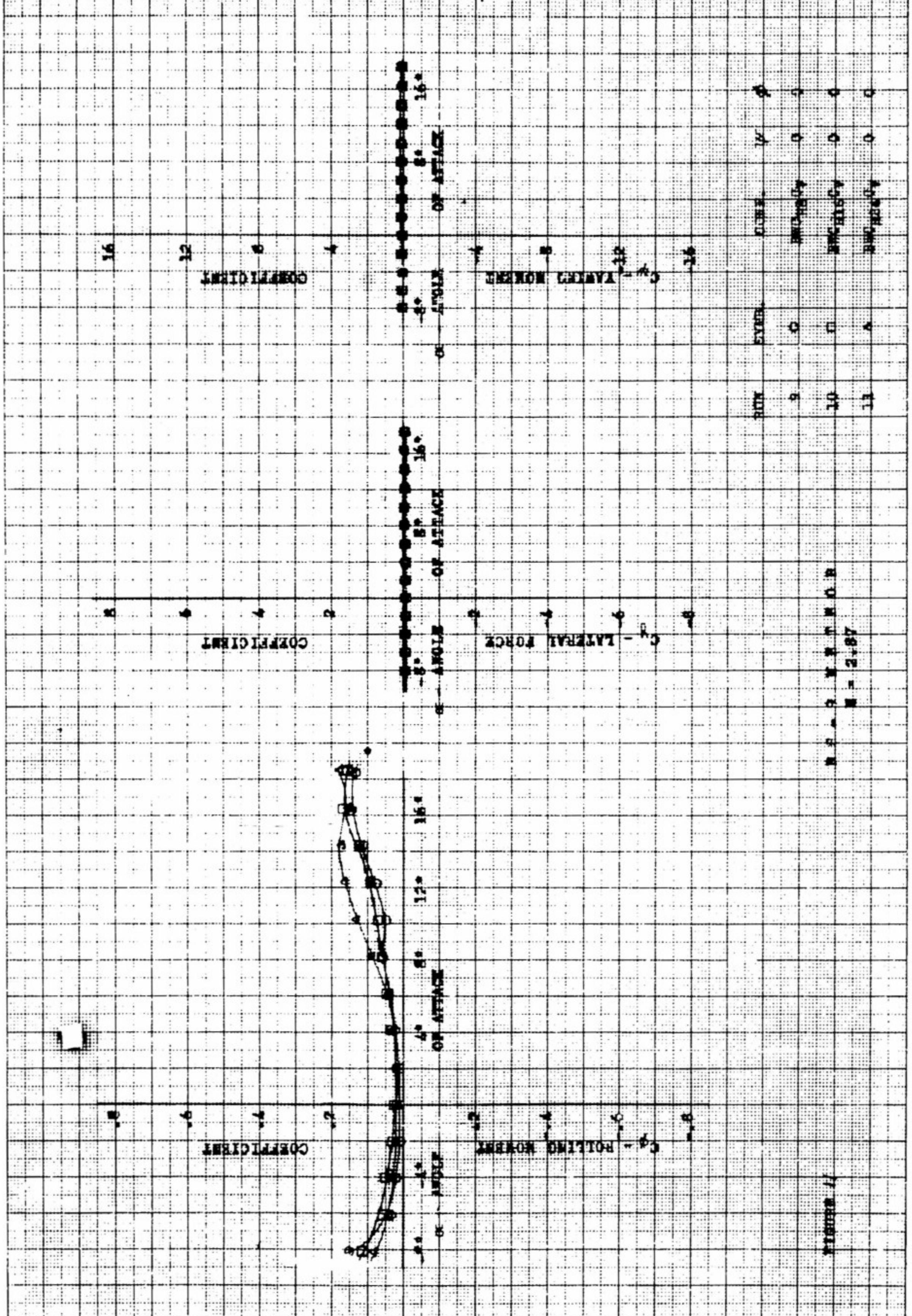
COEFFICIENT
YAWING MOMENT
LATERAL FORCE
ROLLING MOMENT
ANGLE OF ATTACK
RUN
SYMB.
CONF.
M = 2.87
FIGURE 11

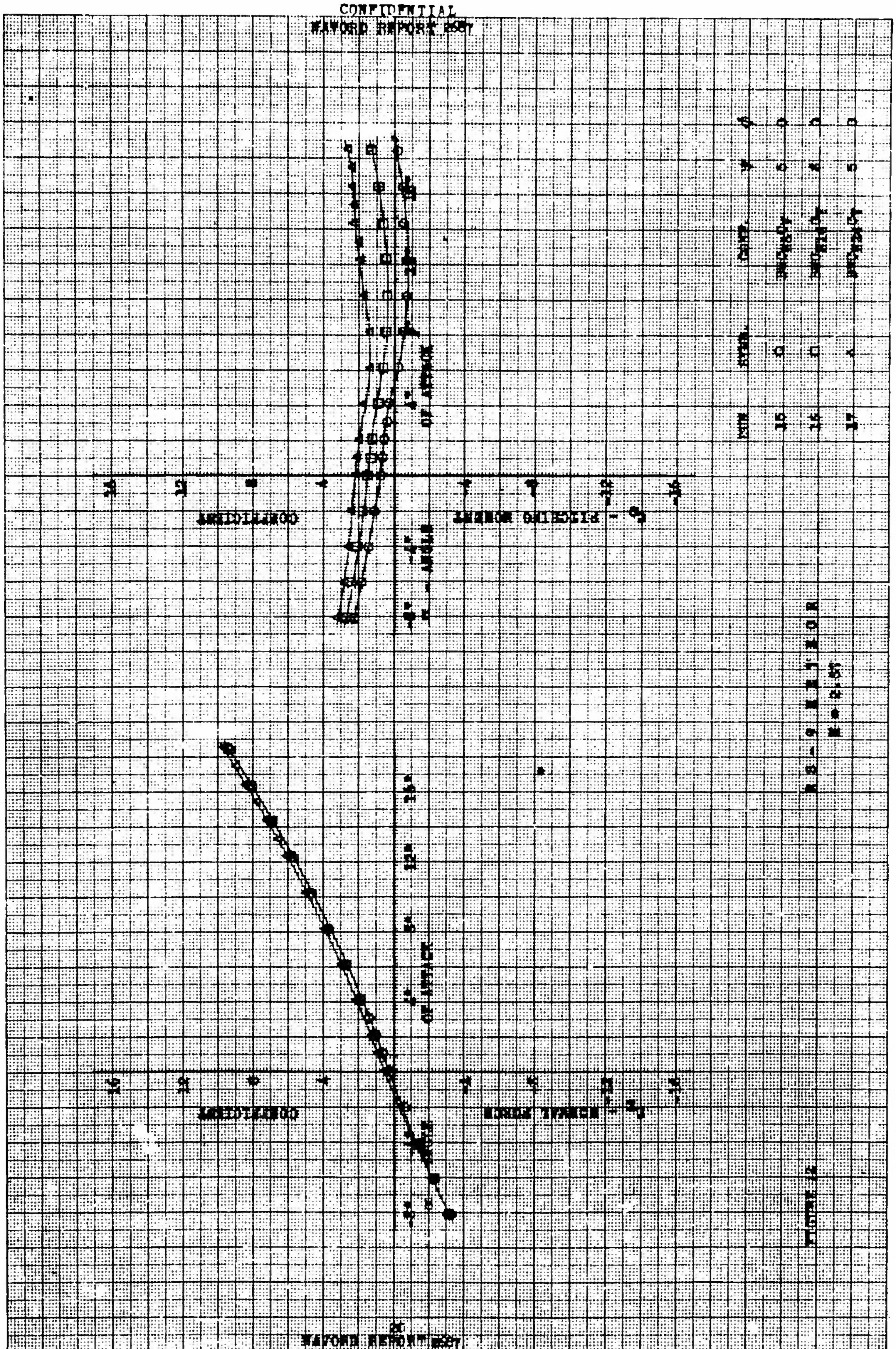

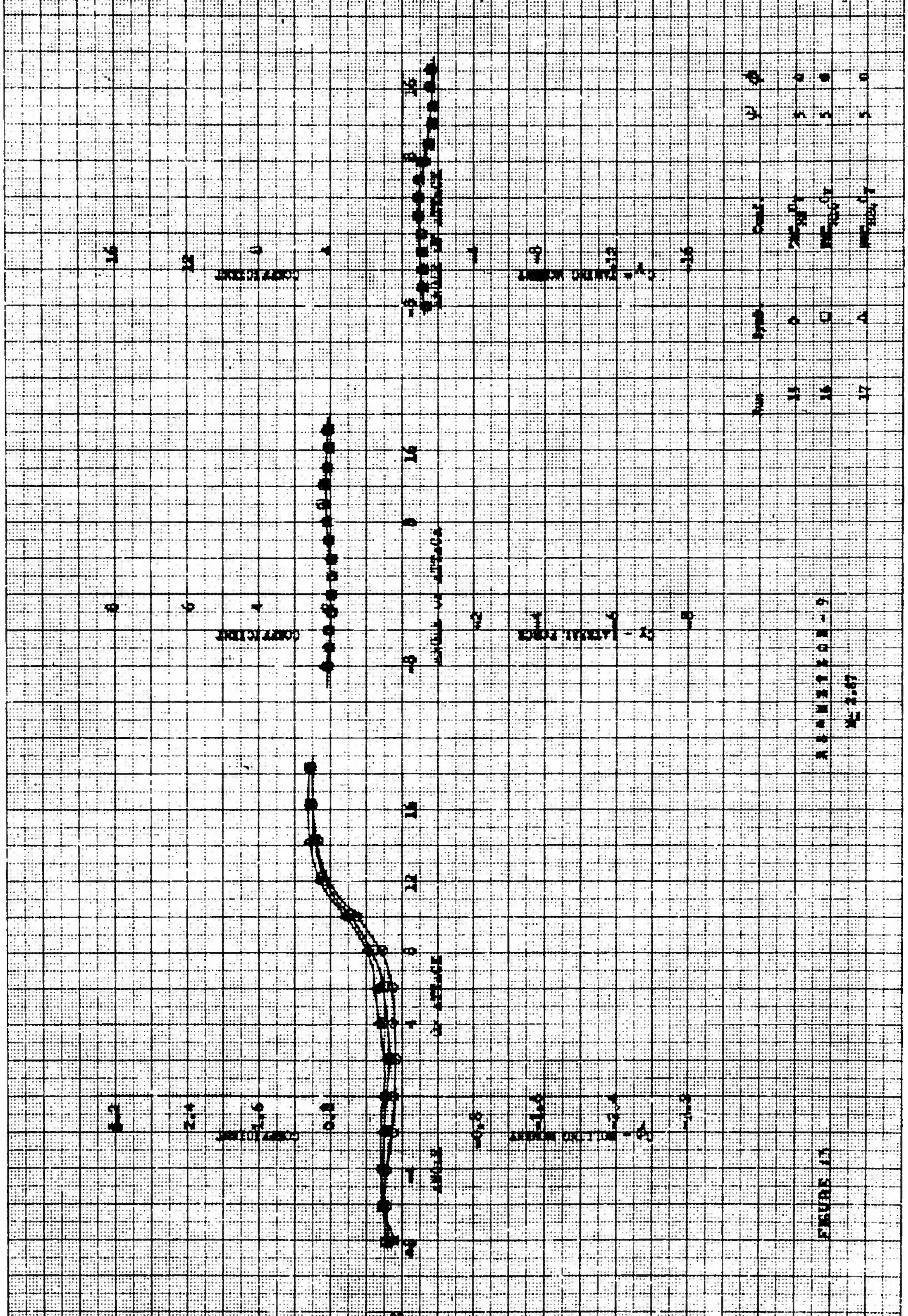
ANGLE OF ATTACK
COEFFICIENT
FIGURE 15

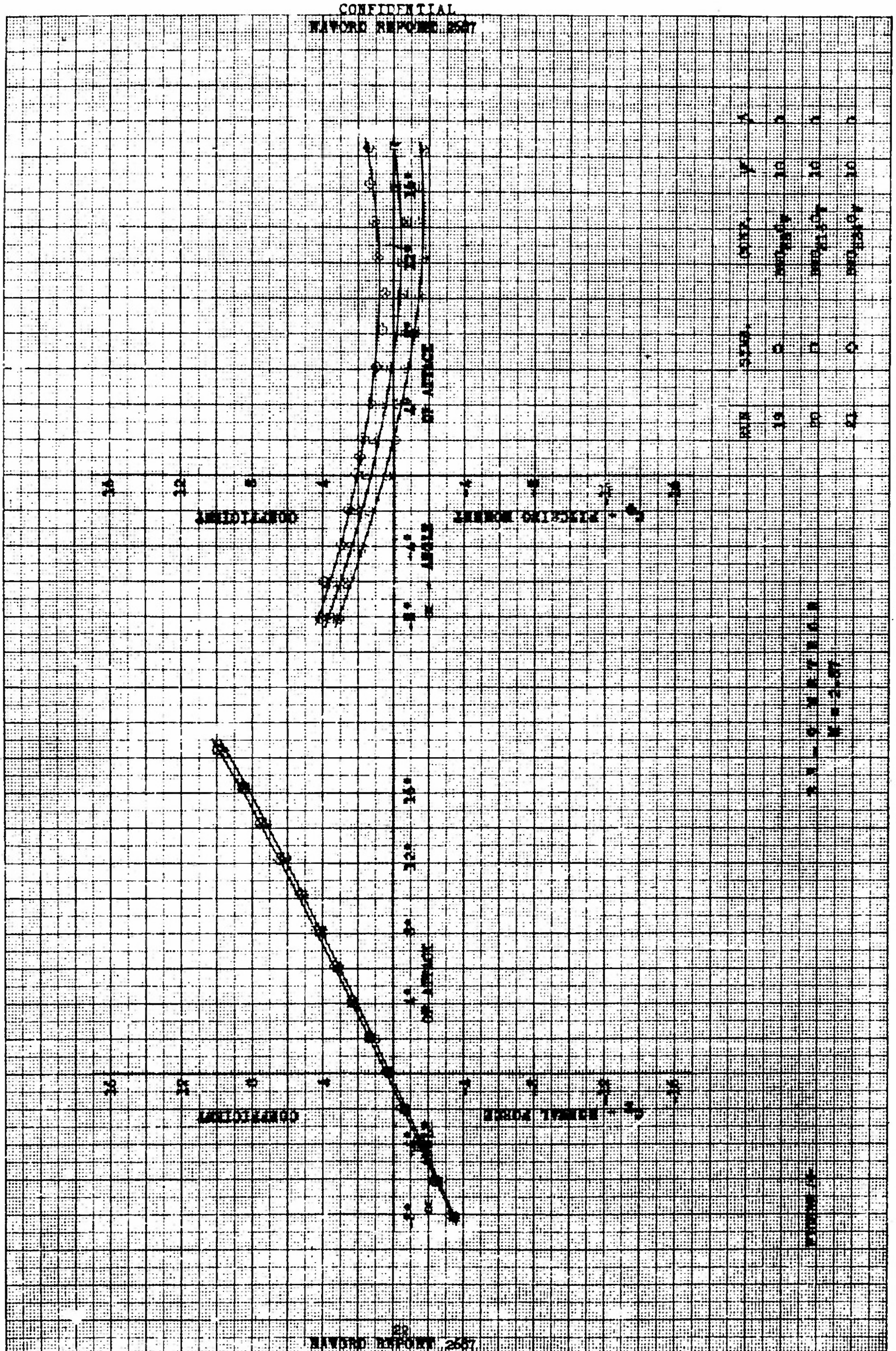

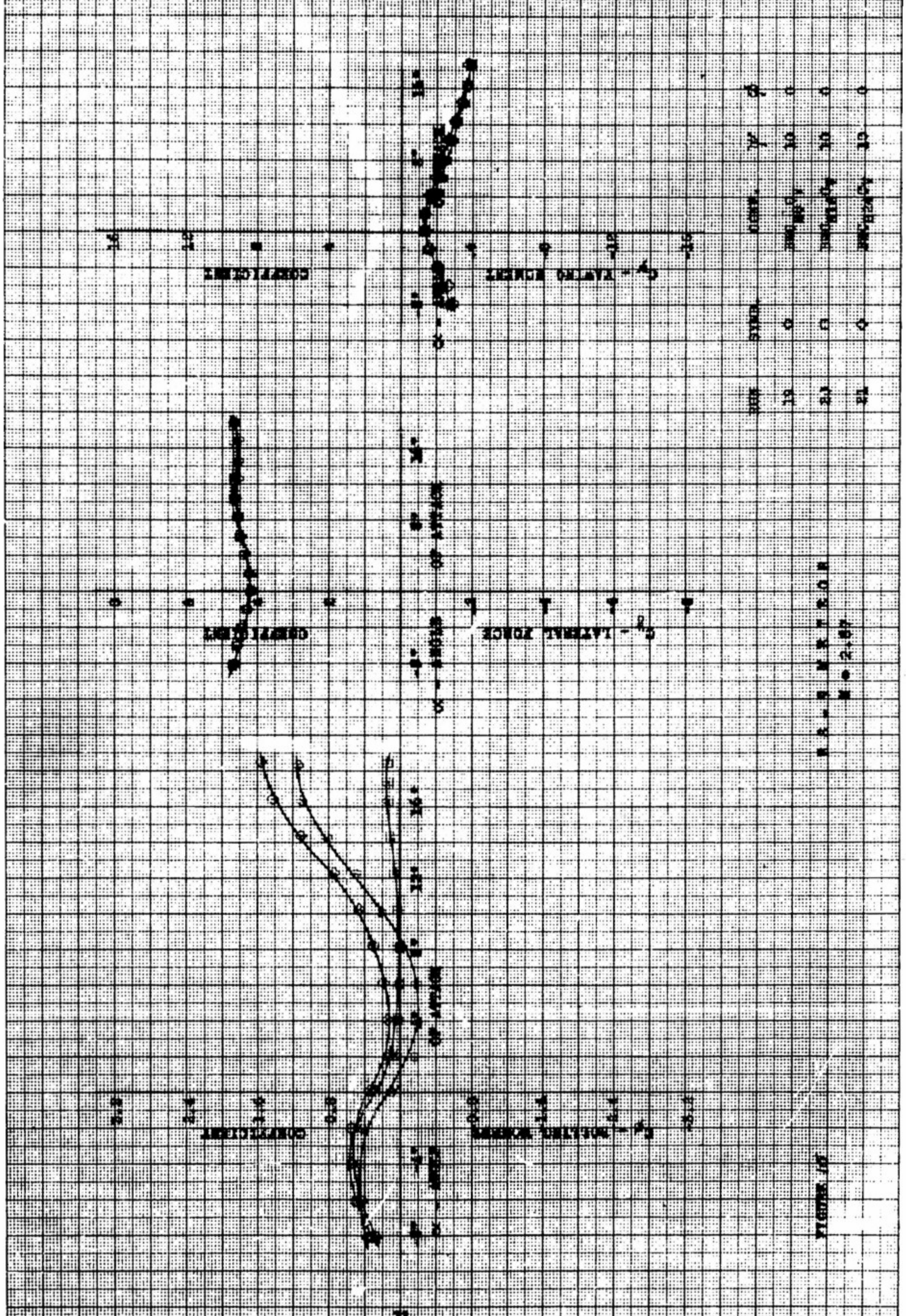
FIGURE 17
M = 2.87
C_n - YAWING MOMENT COEFFICIENT
C_Y - LATERAL FORCE COEFFICIENT
C_l - ROLLING MOMENT COEFFICIENT
ANGLE OF ATTACK

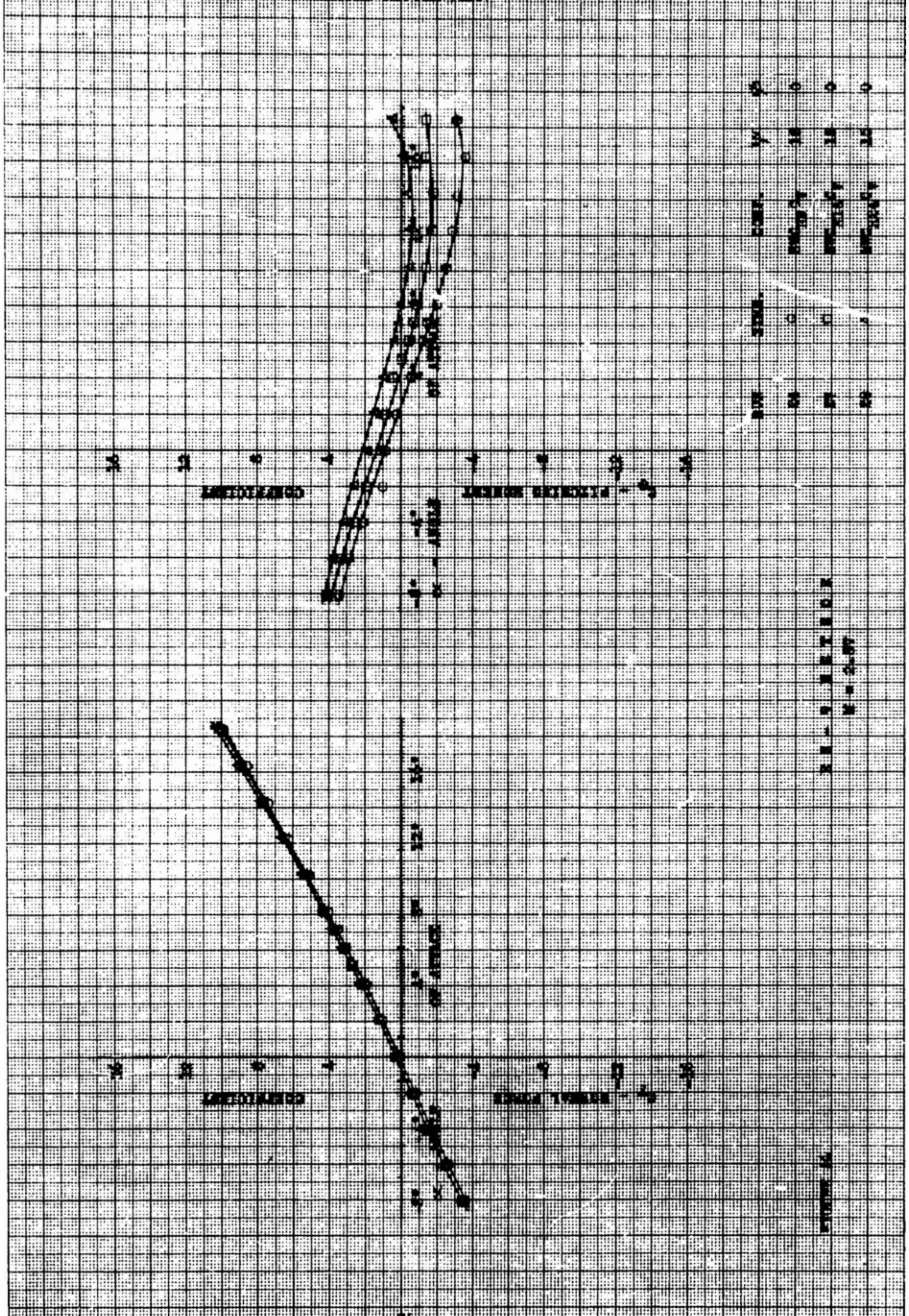

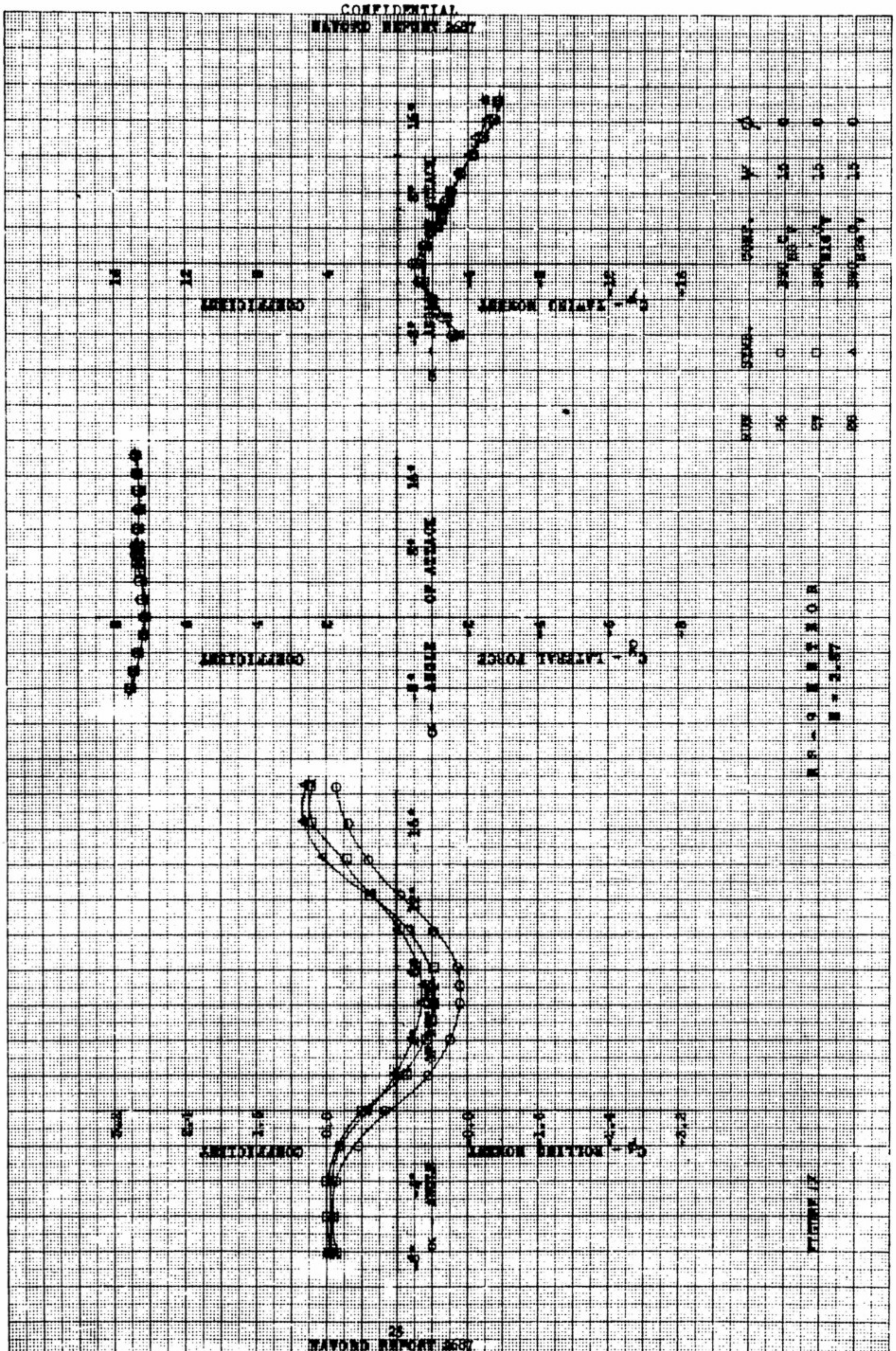
RUN
SYMB.
CONF.
COEFFICIENT
LATERAL FORCE
YAWING MOMENT
ROLLING MOMENT
ANGLE OF ATTACK

FIGURE 17

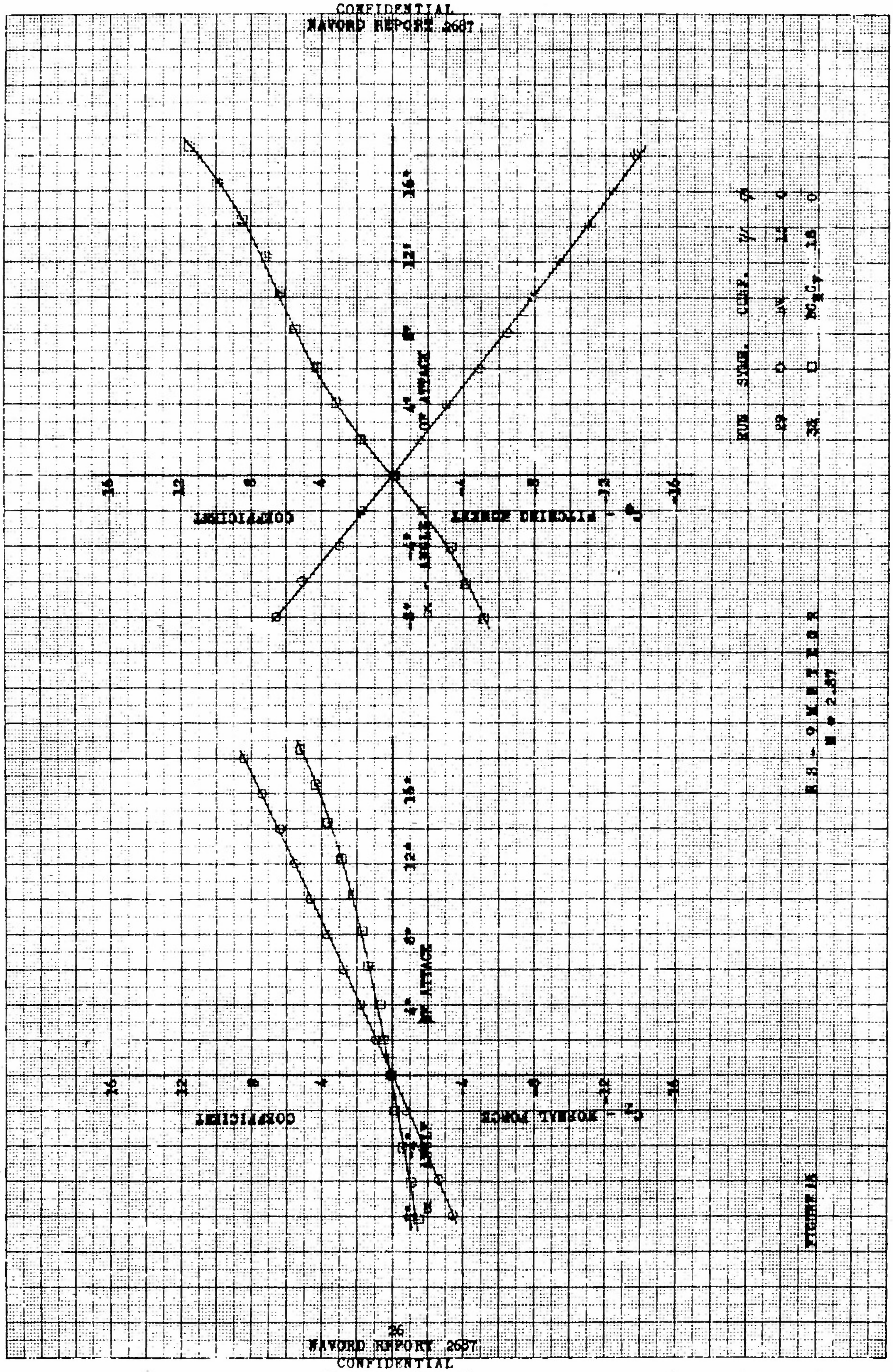

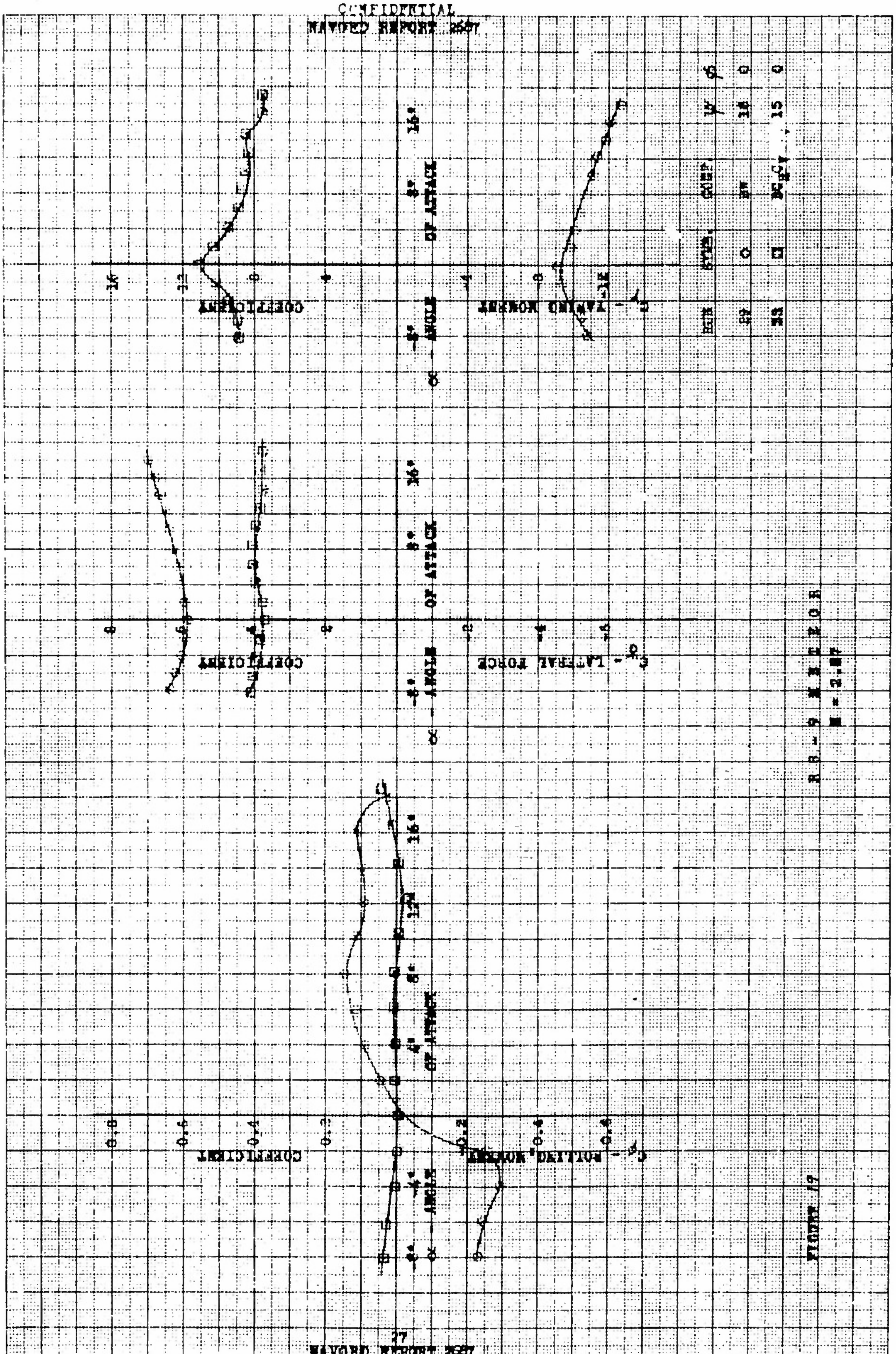

FIGURE 19

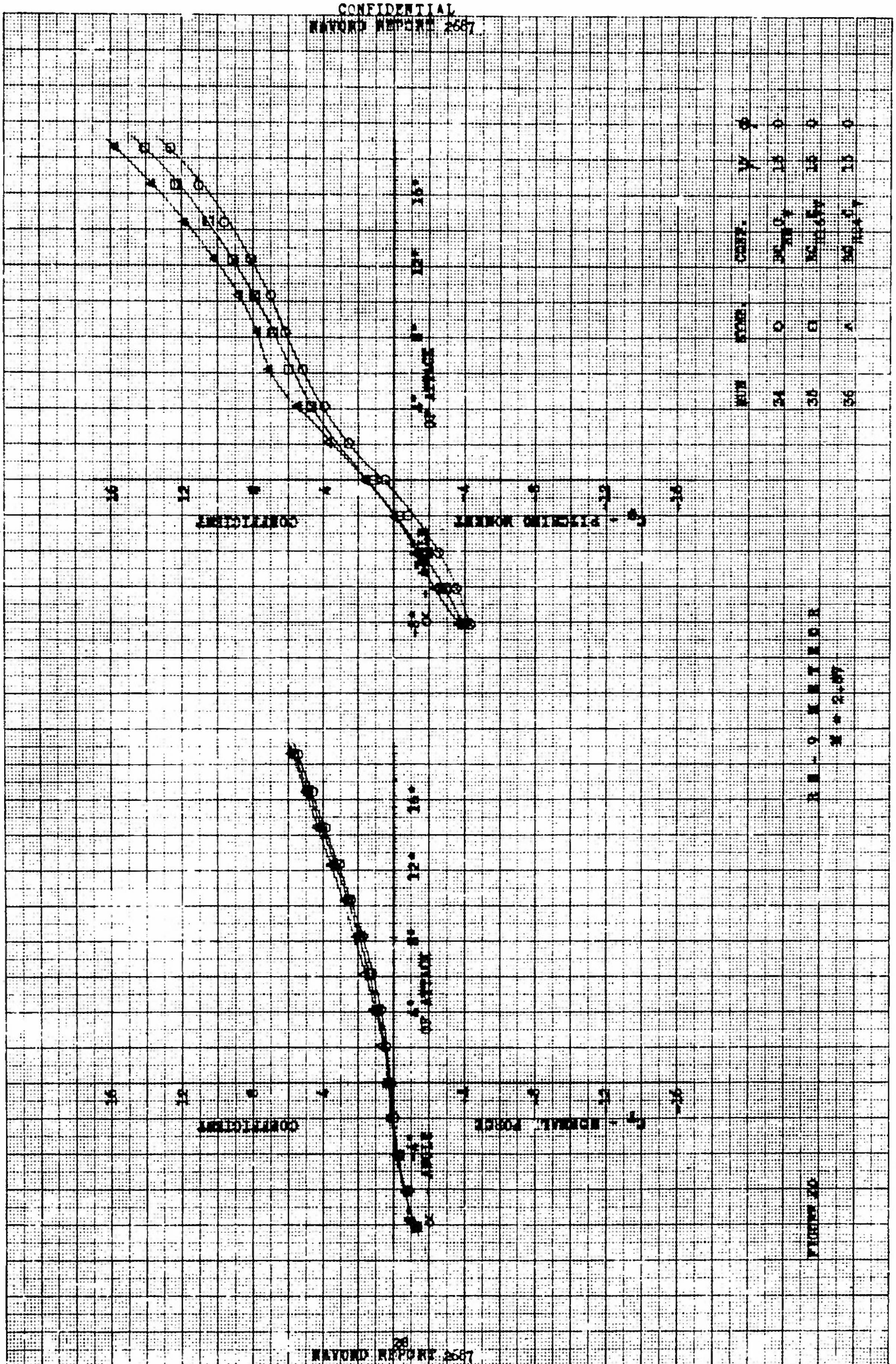

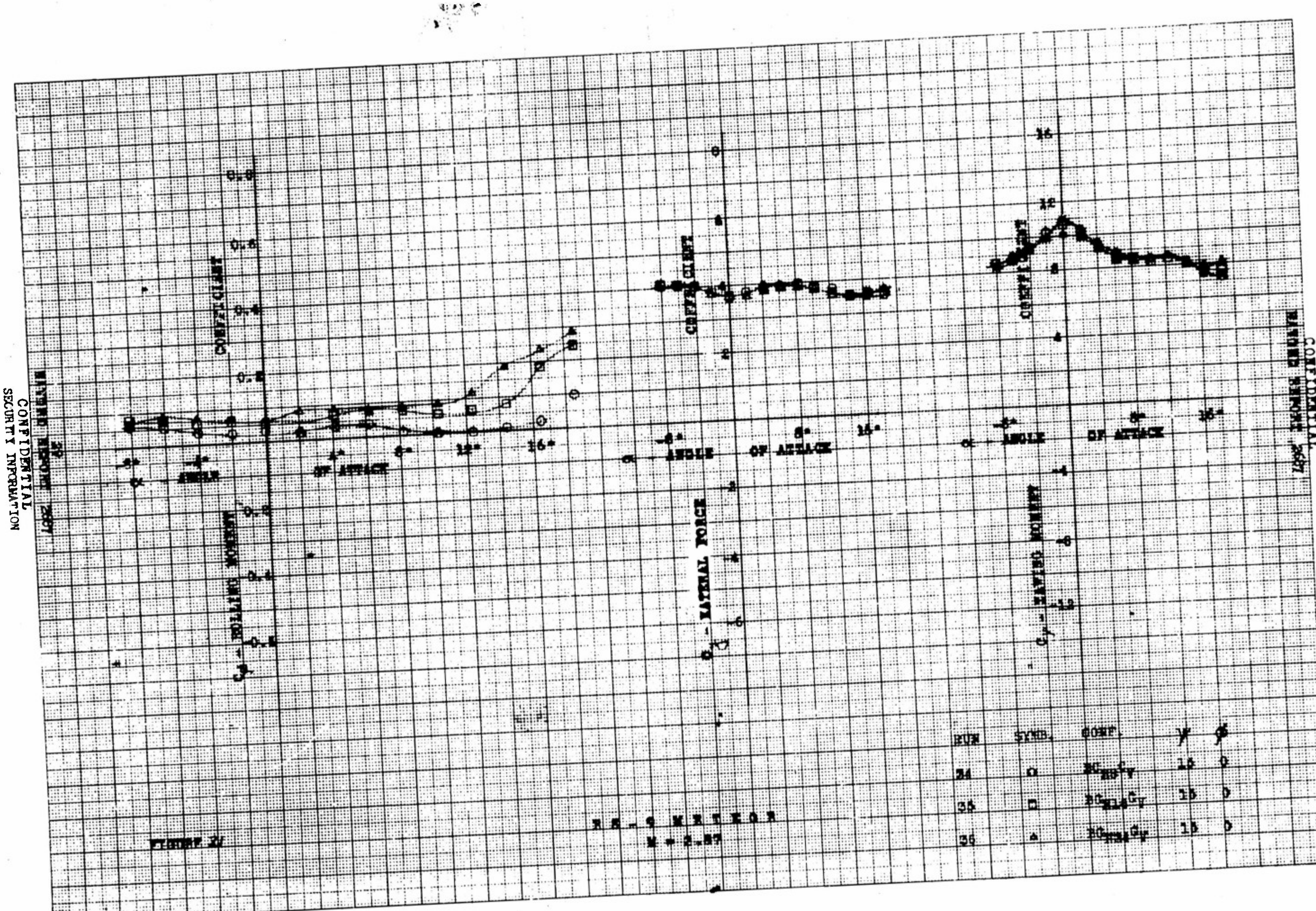
COEFFICIENT
C_l - ROLLING MOMENT
α - ANGLE OF ATTACK
COEFFICIENT
C_Y - LATERAL FORCE
α - ANGLE OF ATTACK
COEFFICIENT
C_n - YAWING MOMENT
α - ANGLE OF ATTACK
RUN SYMB. CONF. ψ ϕ
M = 2.87

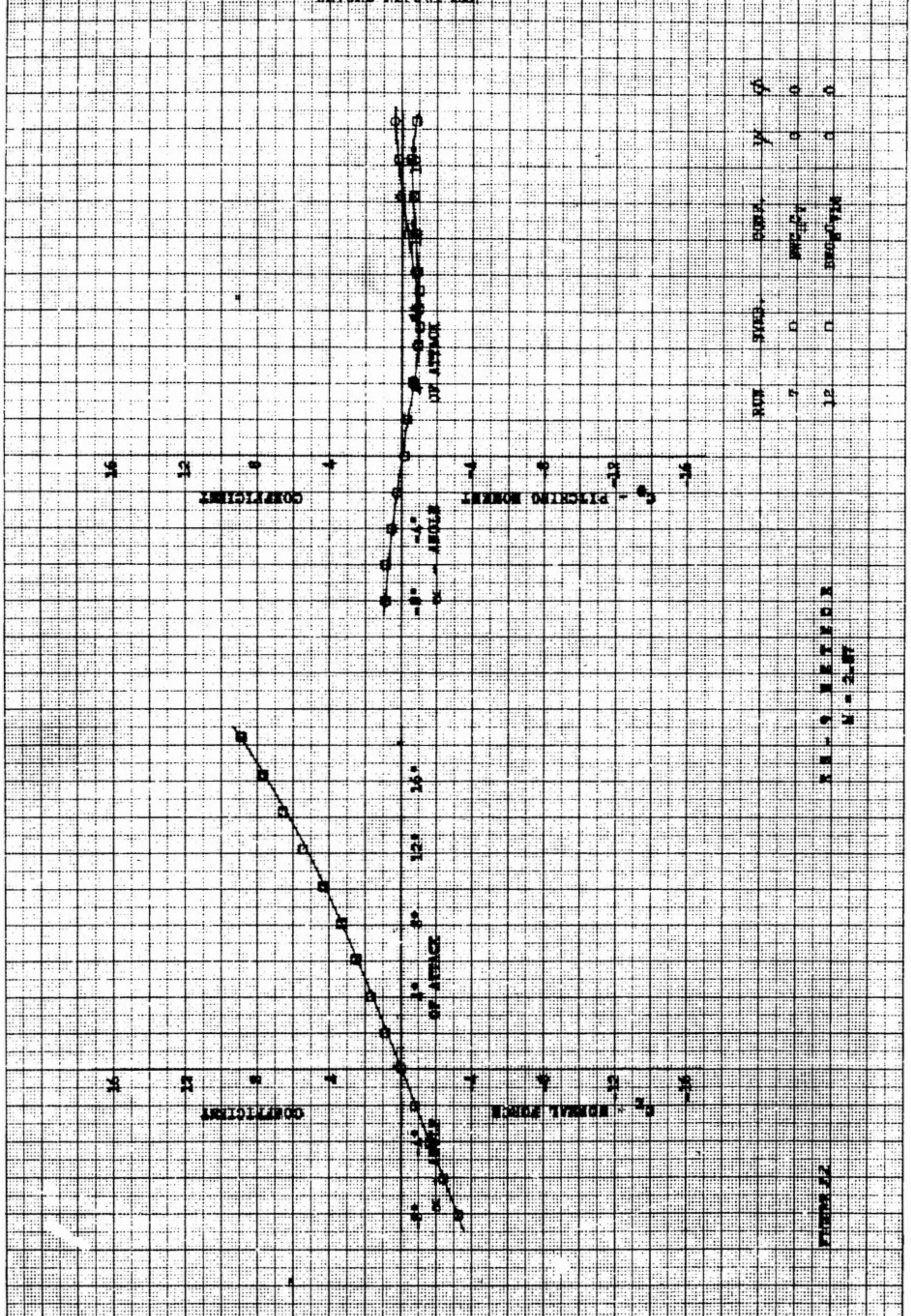
COEFFICIENT
NORMAL FORCE
α - ANGLE OF ATTACK
COEFFICIENT
PITCHING MOMENT
α - ANGLE OF ATTACK
RUN
SYMB.
CONF.
ψ
φ
7
0
0
12
0
0

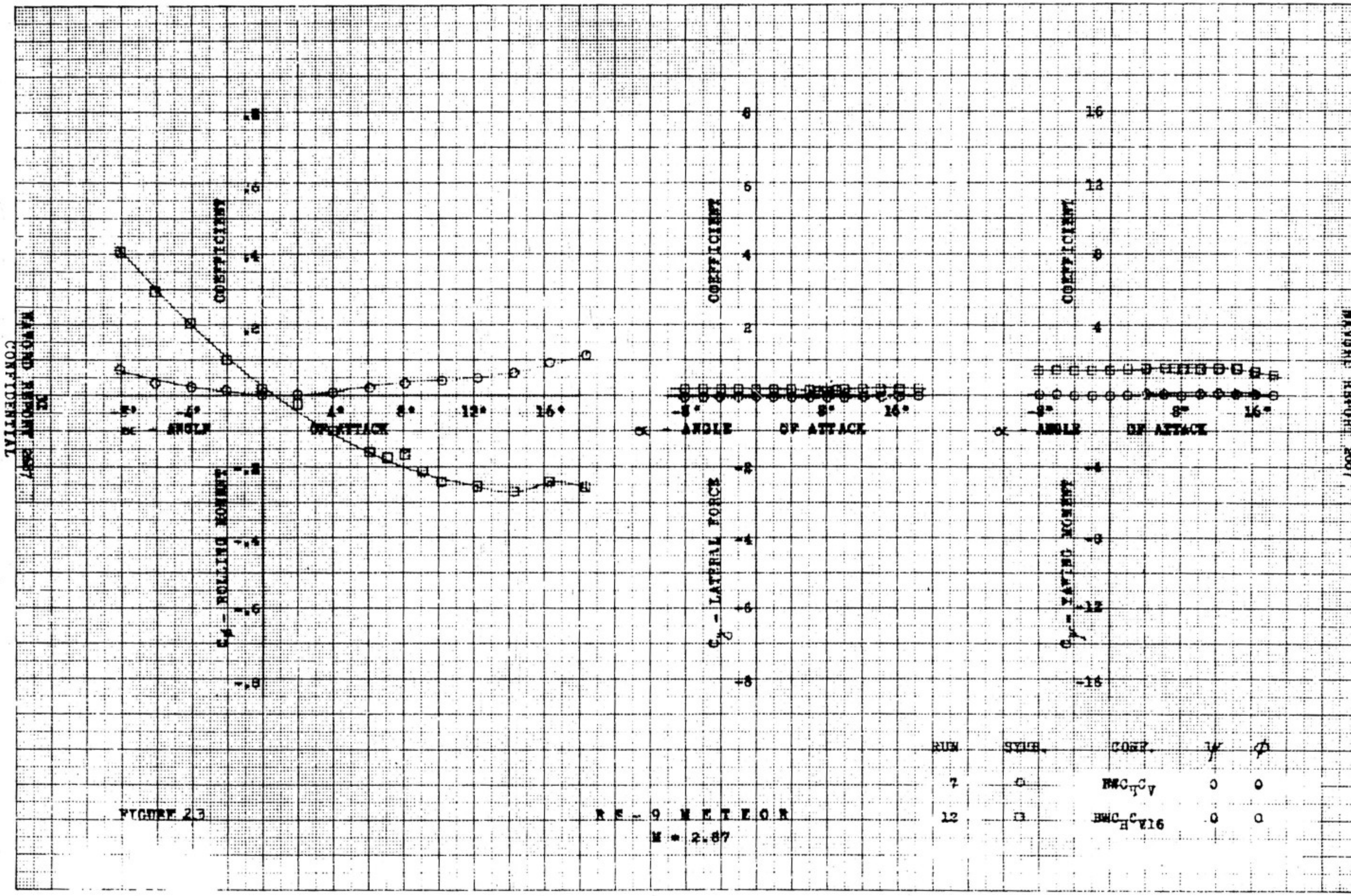

FIGURE 23

RE - 9 METEOR
M = 2.87

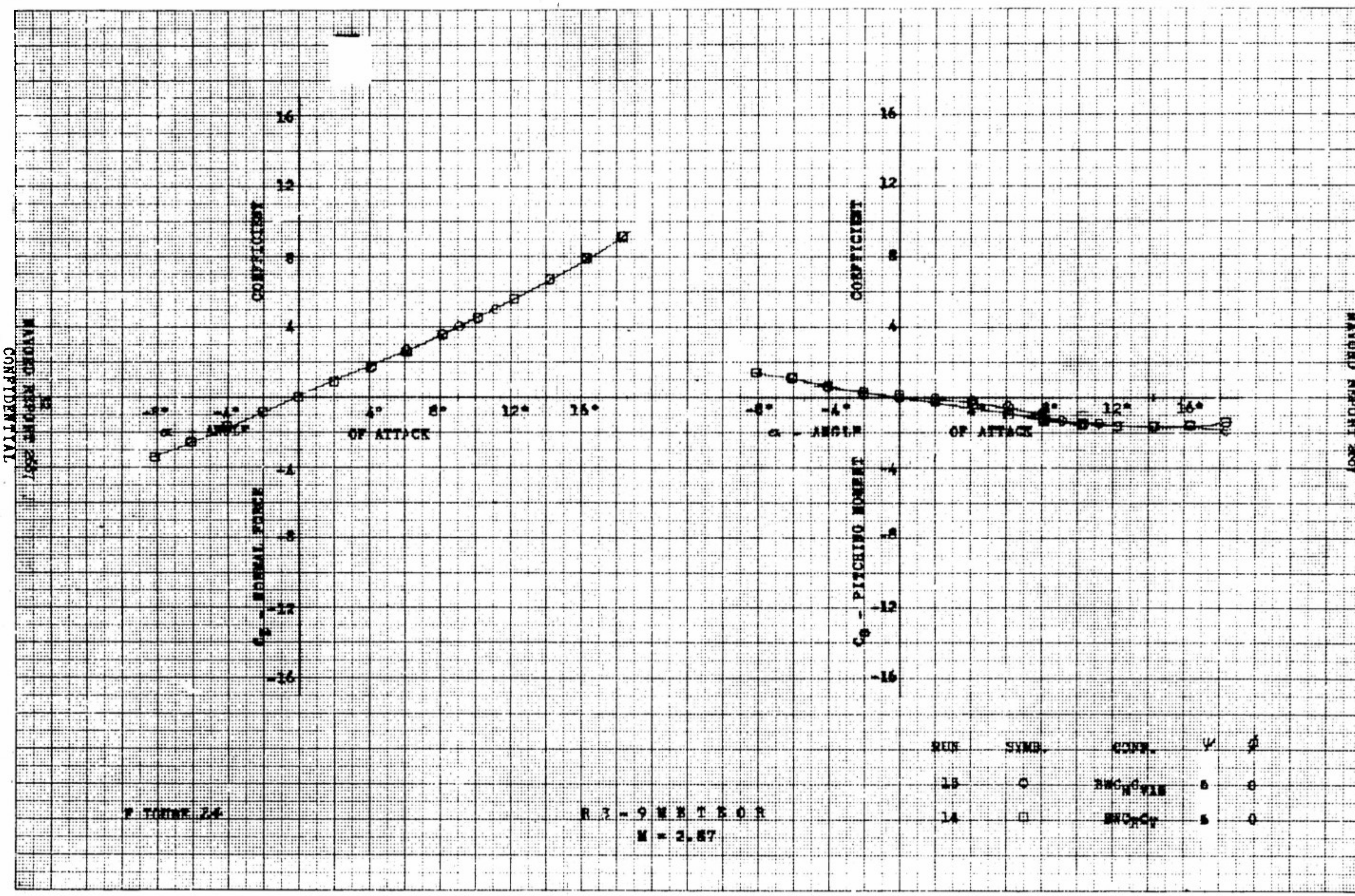
C_N - NORMAL FORCE COEFFICIENT
α - ANGLE OF ATTACK
C_m - PITCHING MOMENT COEFFICIENT
α - ANGLE OF ATTACK
16
12
8
4
-4
-8
-12
-16
-8°
-4°
4°
8°
12°
16°
RUN SYMB. CONF. ψ ϕ
15 ○ $BNC_N C_{VIB}$ 6 0
14 □ $BNC_N C_V$ 6 0
R 3 - 9 M E T E O R
M = 2.87

FIGURE 26

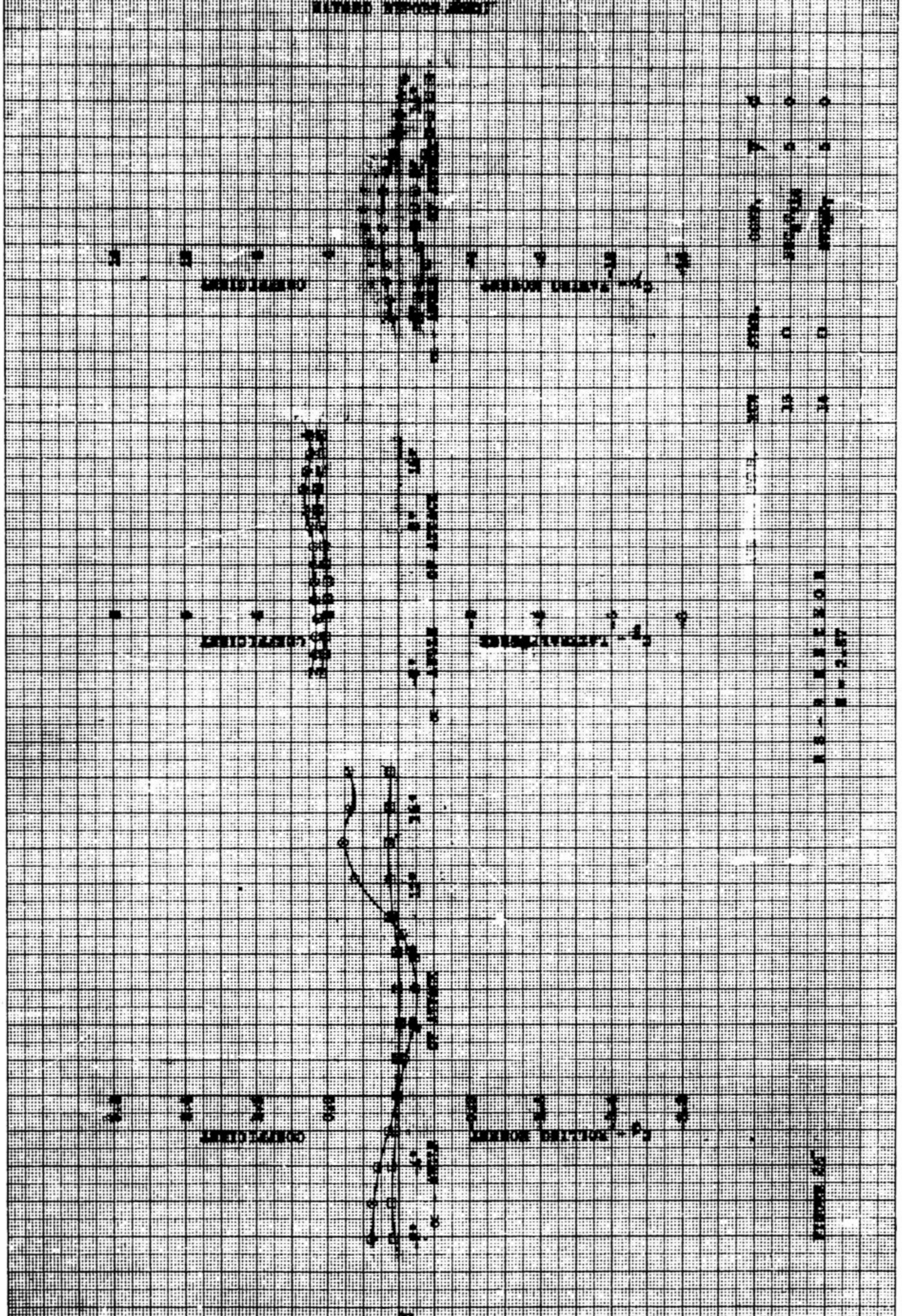

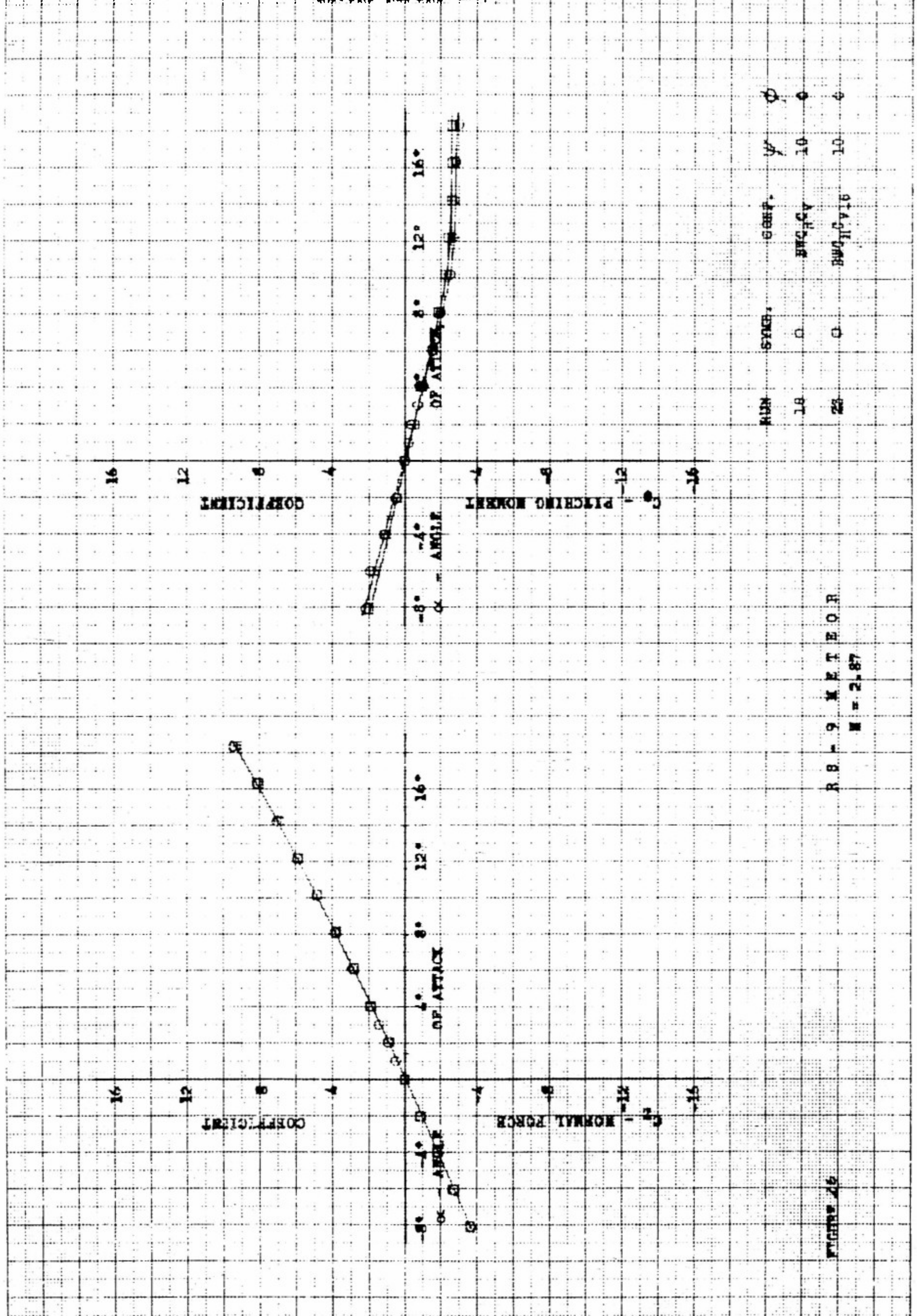
PITCHING MOMENT COEFFICIENT
NORMAL FORCE COEFFICIENT
ANGLE OF ATTACK
RUN
SYMB.
CONF.
RB - 9 METEOR
M = 2.87

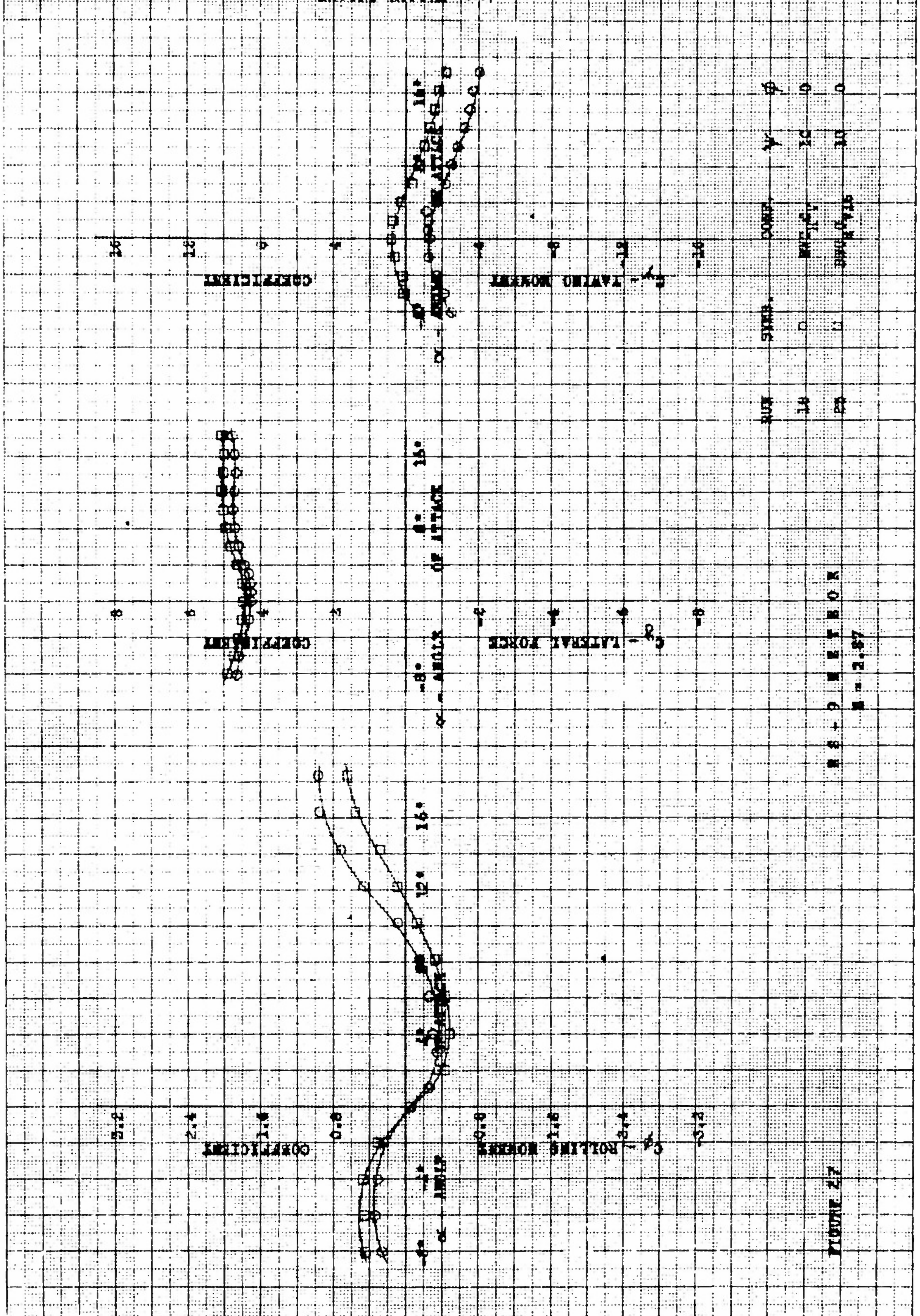
YAWING MOMENT COEFFICIENT
LATERAL FORCE COEFFICIENT
ROLLING MOMENT COEFFICIENT
ANGLE OF ATTACK
NS-9 METEOR
M = 2.87

FIGURE 27

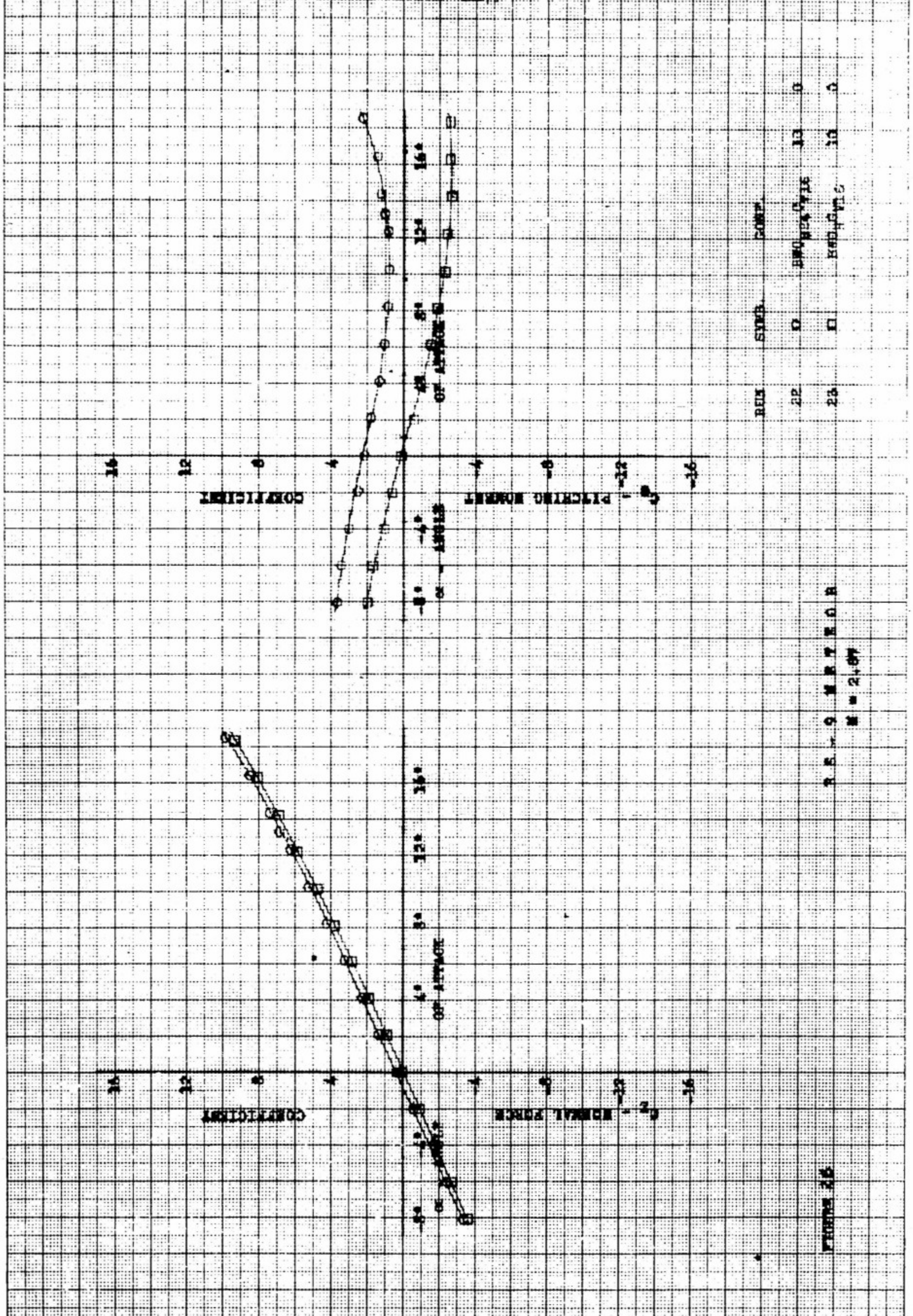
COEFFICIENT
C_N - NORMAL FORCE
α - ANGLE OF ATTACK
COEFFICIENT
C_m - PITCHING MOMENT
RUN SYMB. CONF.
22
23
FIGURE 26
METEOR

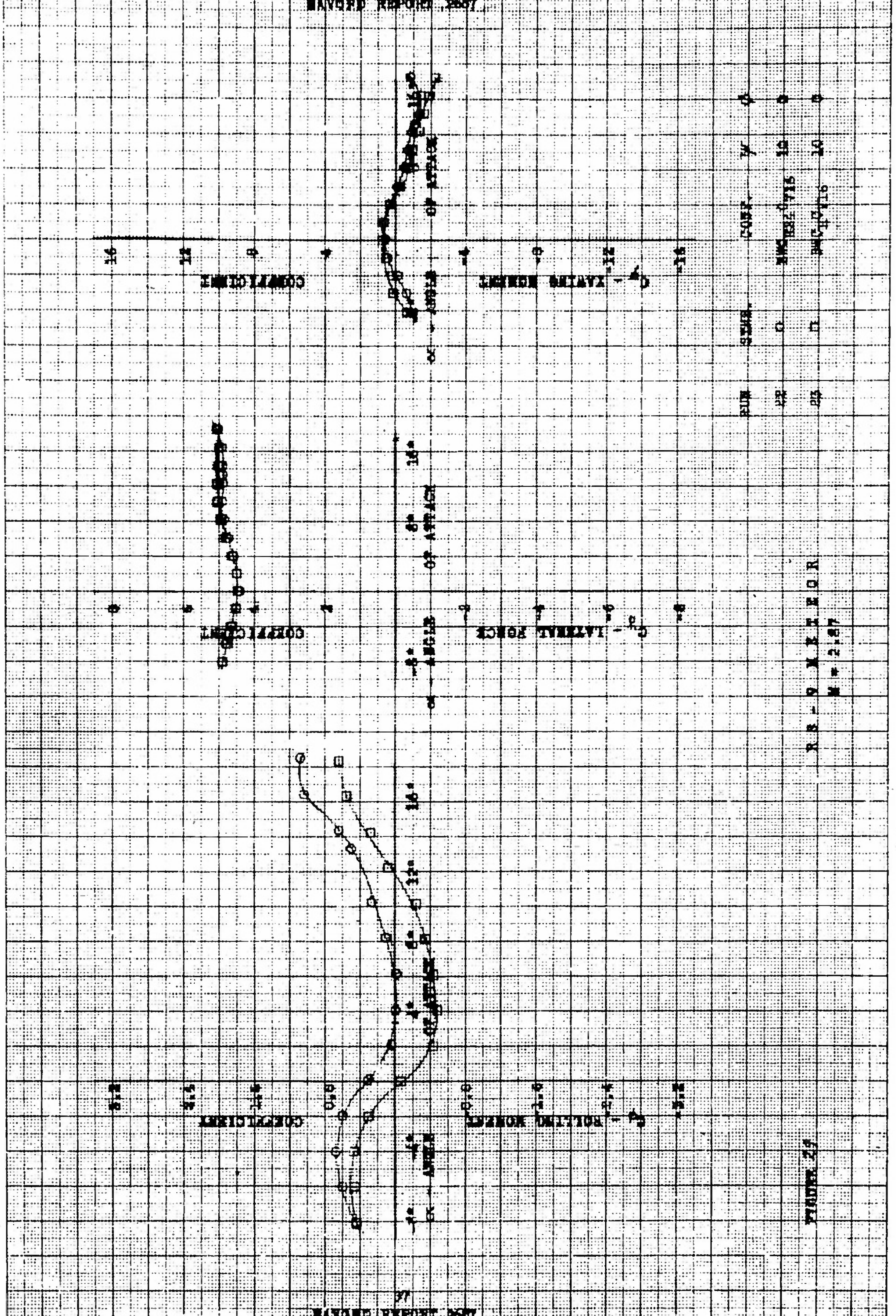

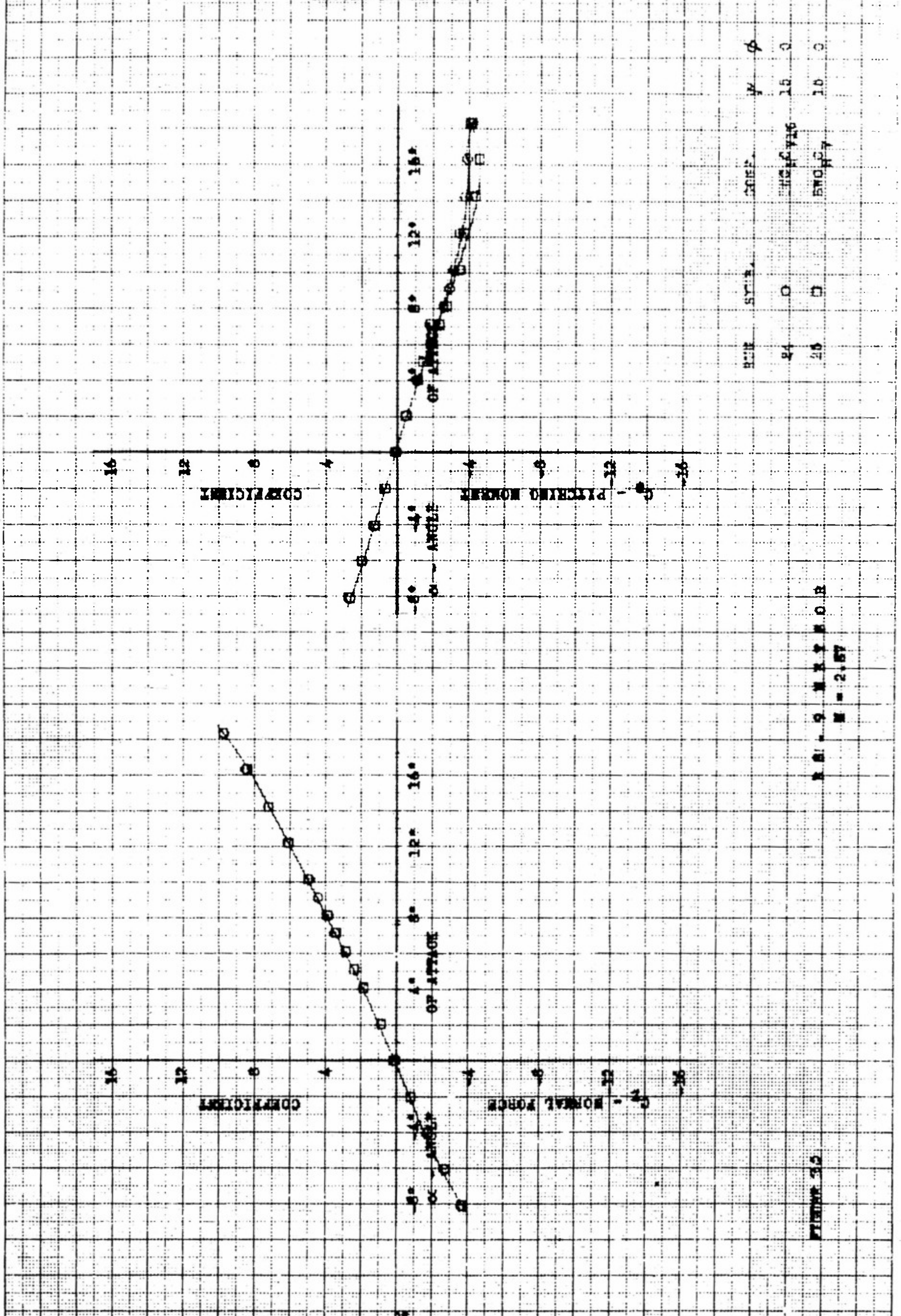
PITCHING MOMENT COEFFICIENT
NORMAL FORCE COEFFICIENT
ANGLE OF ATTACK
M = 2.87

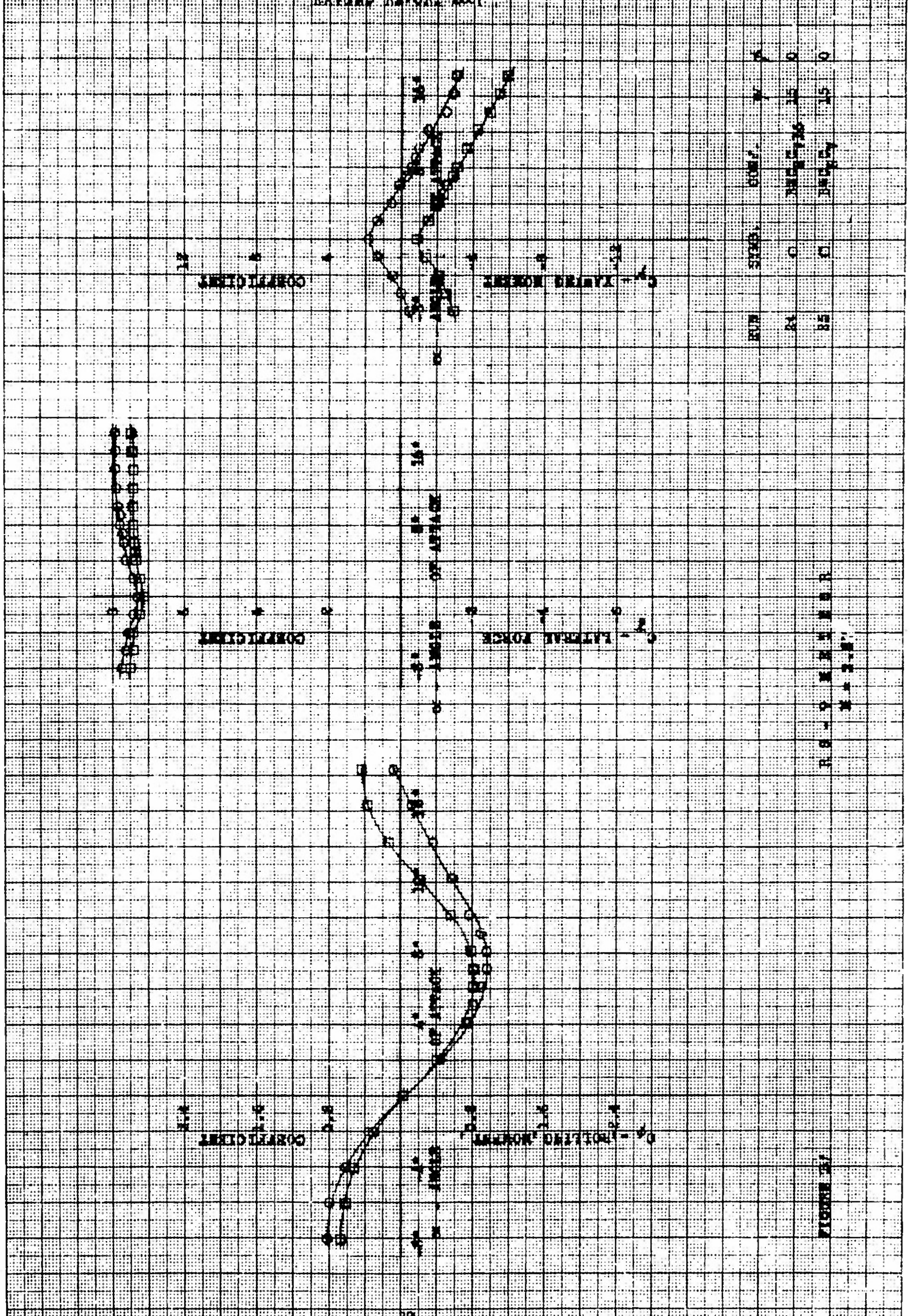

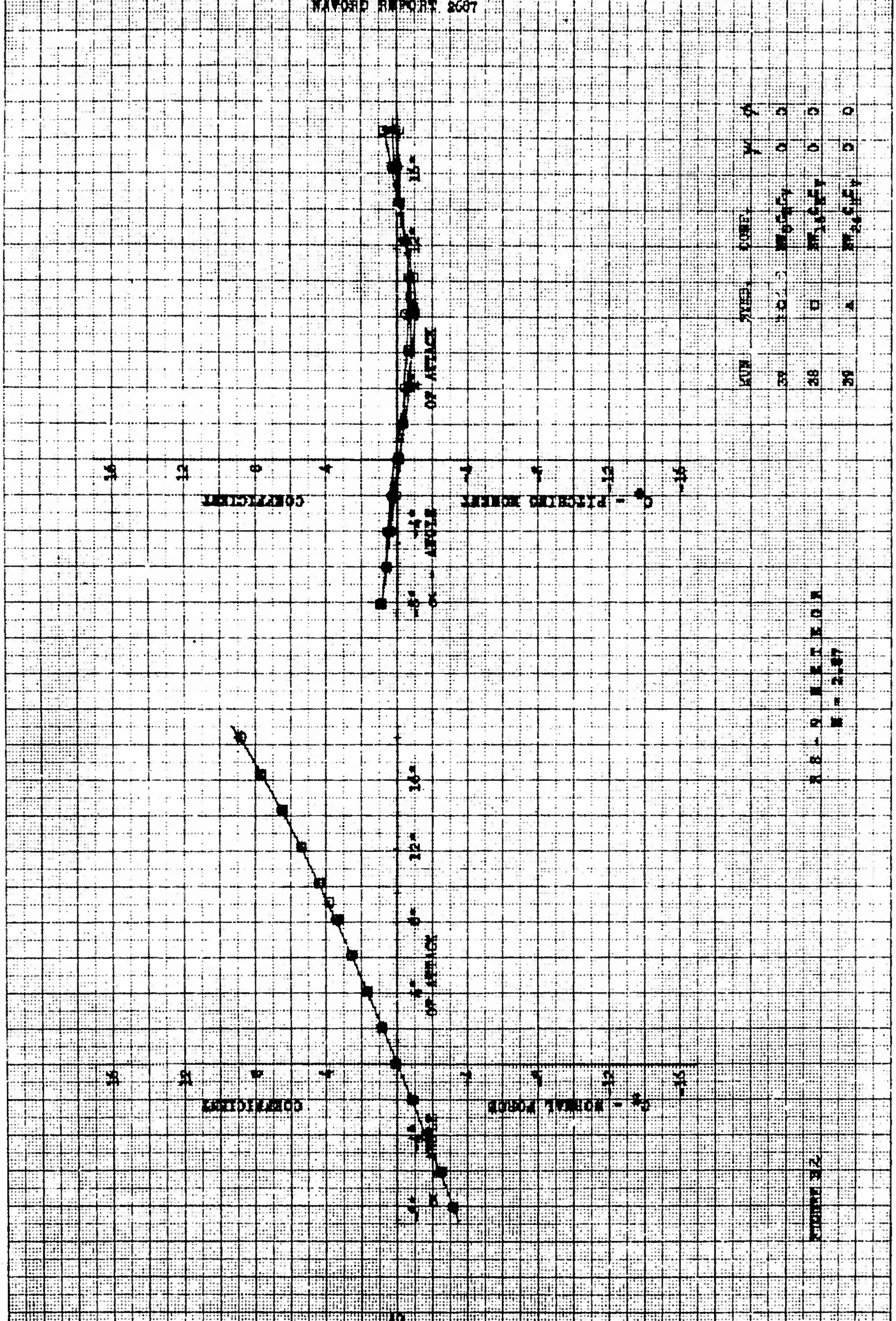

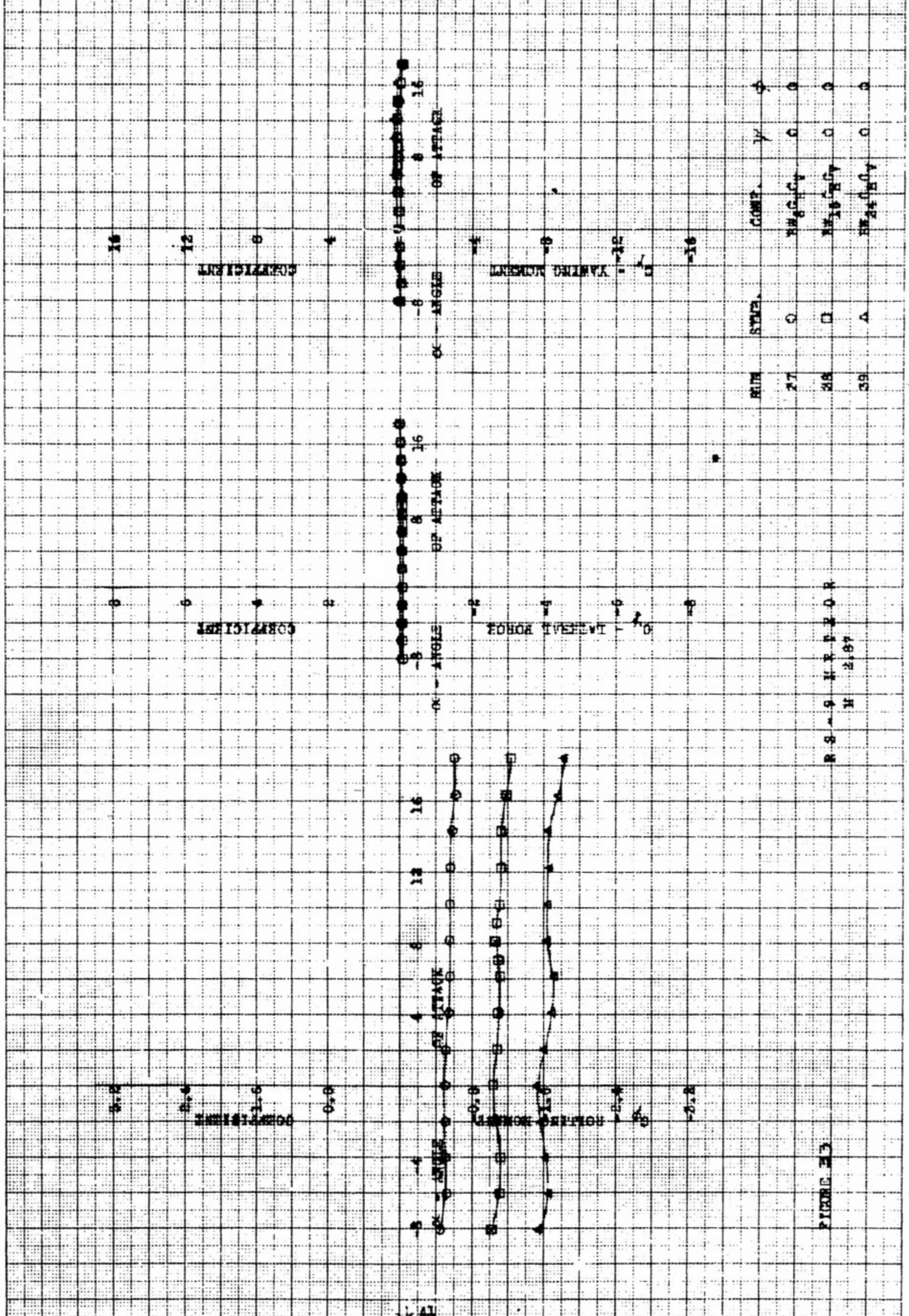

FIGURE 33

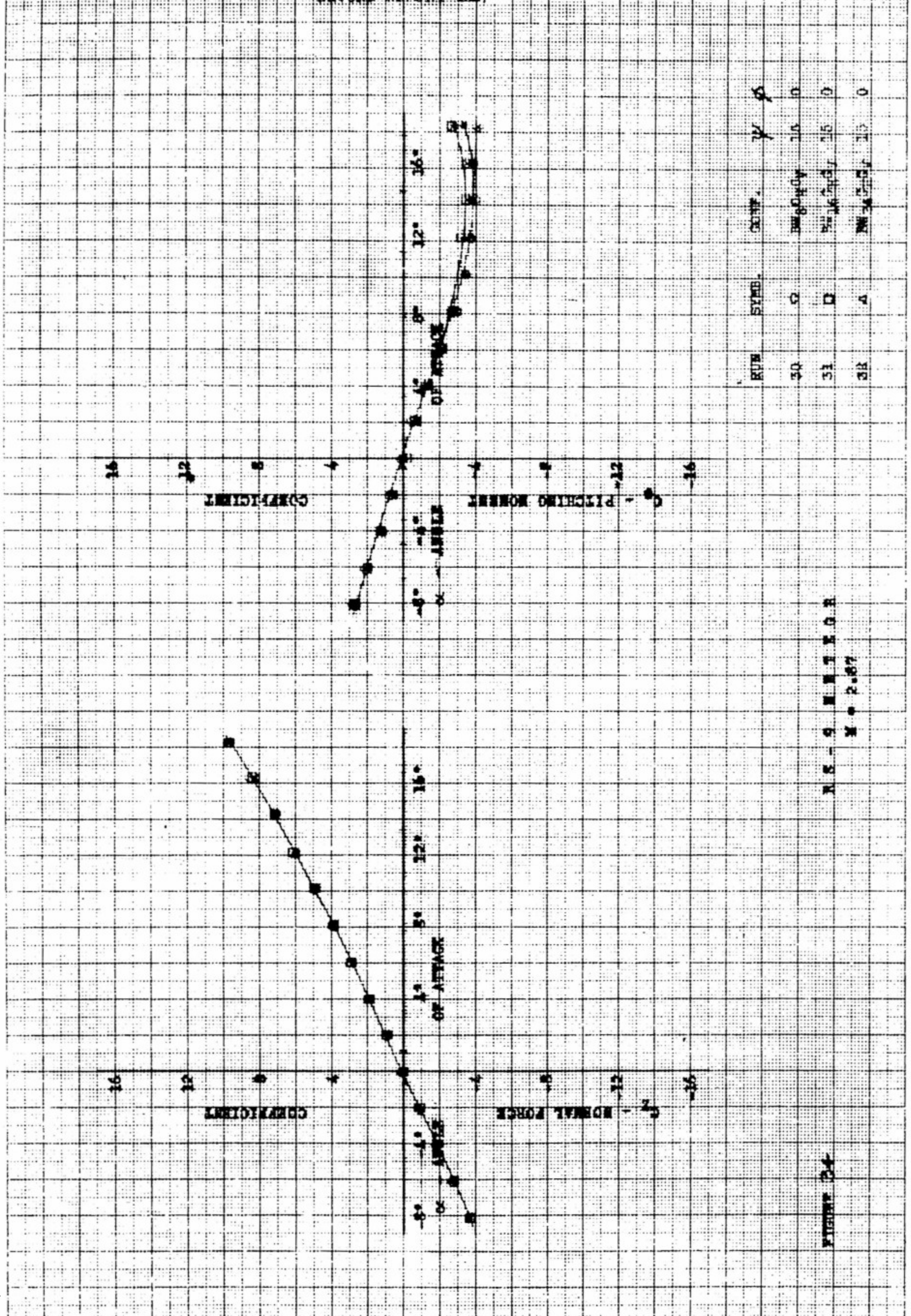
C_m - PITCHING MOMENT COEFFICIENT
C_N - NORMAL FORCE COEFFICIENT
α - ANGLE OF ATTACK
RUN
SYMB.
CONF.
30
31
32
M = 2.87

FIGURE 24

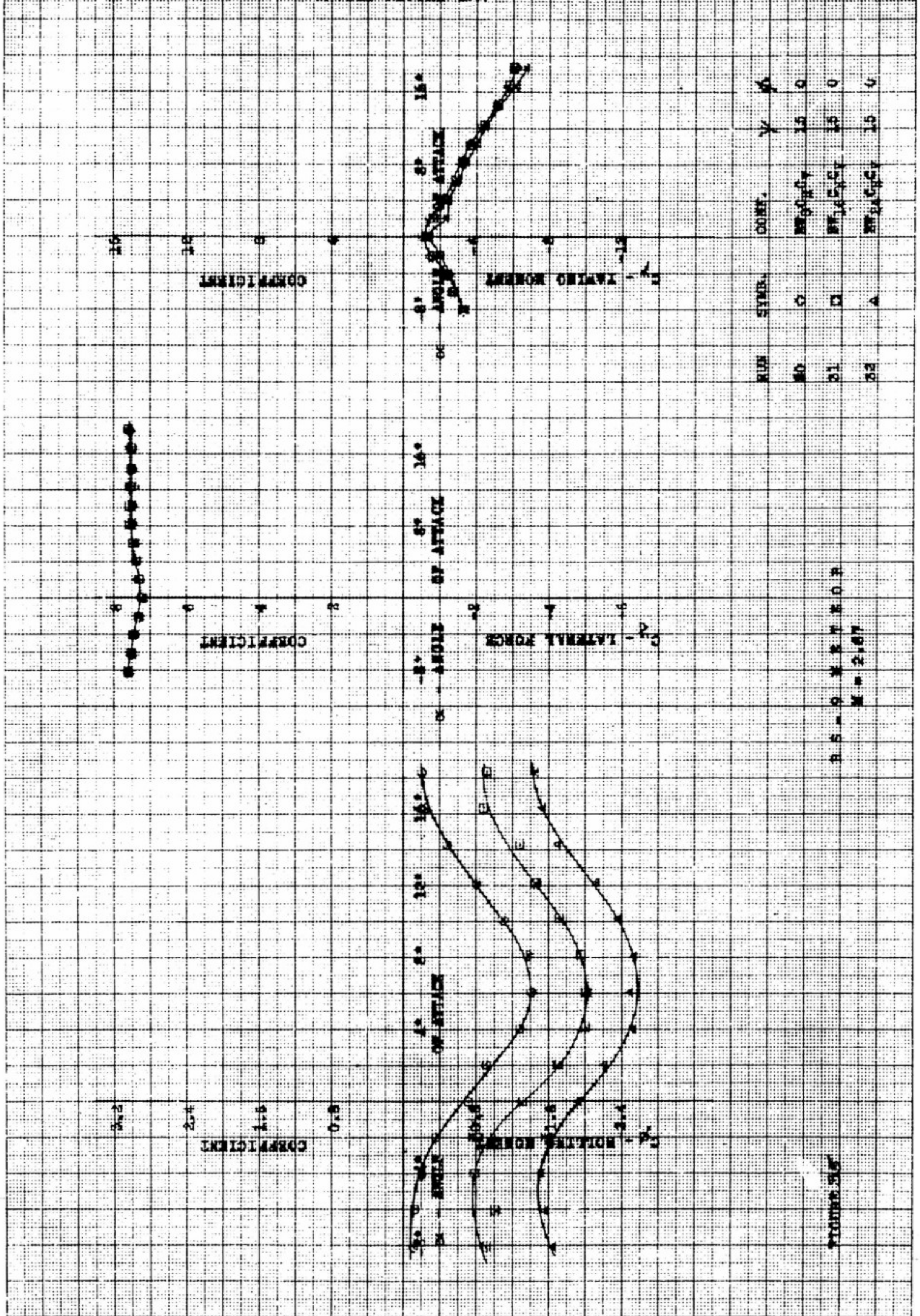

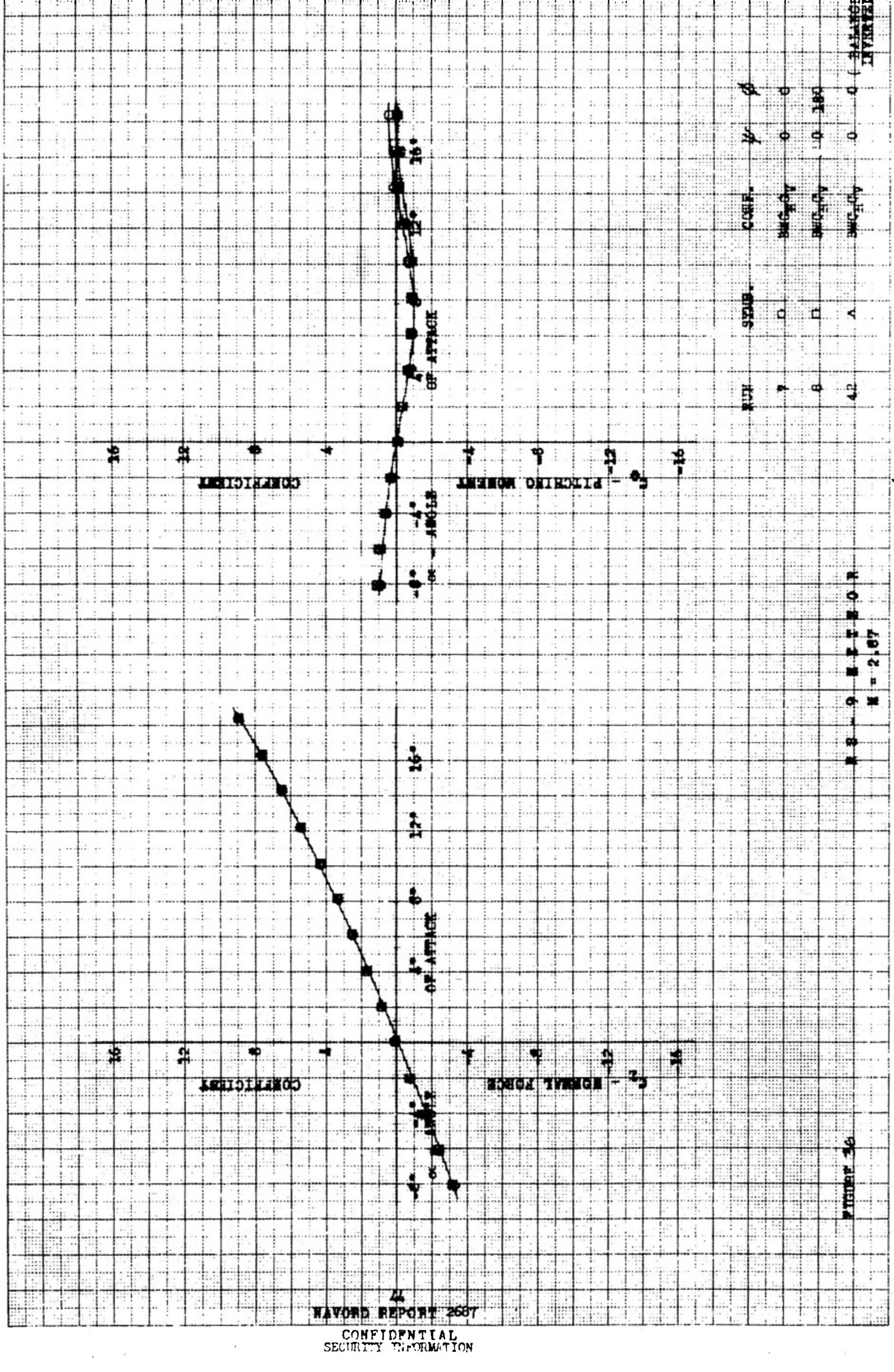
C_m - PITCHING MOMENT COEFFICIENT
C_N - NORMAL FORCE COEFFICIENT
α - ANGLE OF ATTACK
RB-9 METEOR
M = 2.87
RUN
SYMB.
COEF.
ψ
φ
BALANCE INVERTED

FIGURE 36

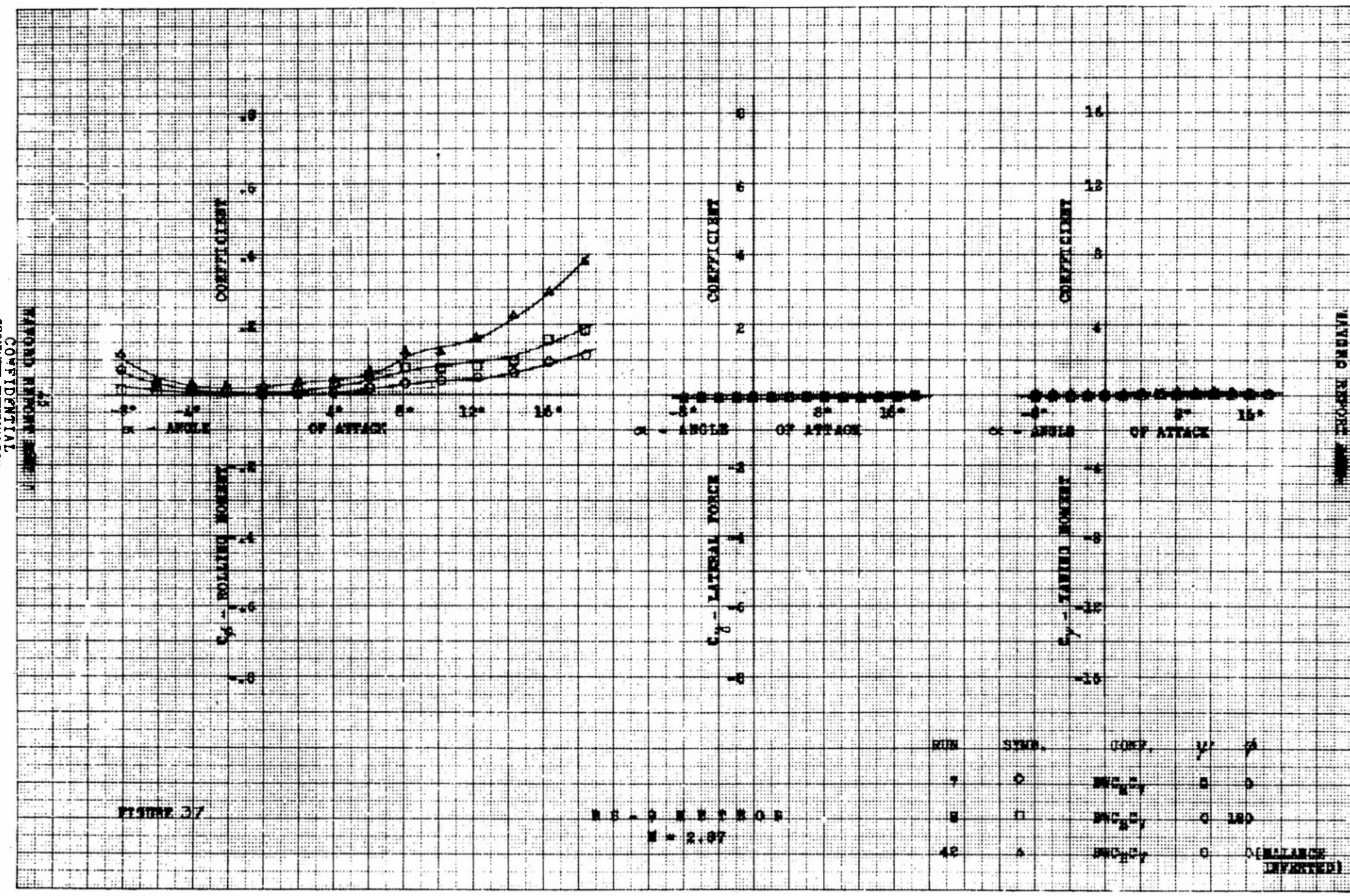
COEFFICIENT
C_{ℓ} - ROLLING MOMENT
α - ANGLE OF ATTACK
COEFFICIENT
C_Y - LATERAL FORCE
α - ANGLE OF ATTACK
COEFFICIENT
C_{n} - YAWING MOMENT
α - ANGLE OF ATTACK
RUN SYMB. CONF. ψ φ
BS - 9 METROS
M = 2.87
(BALANCE INVERTED)

FIGURE 37

REPRESENTATIVE SCHLIEREN PHOTOGRAPHS

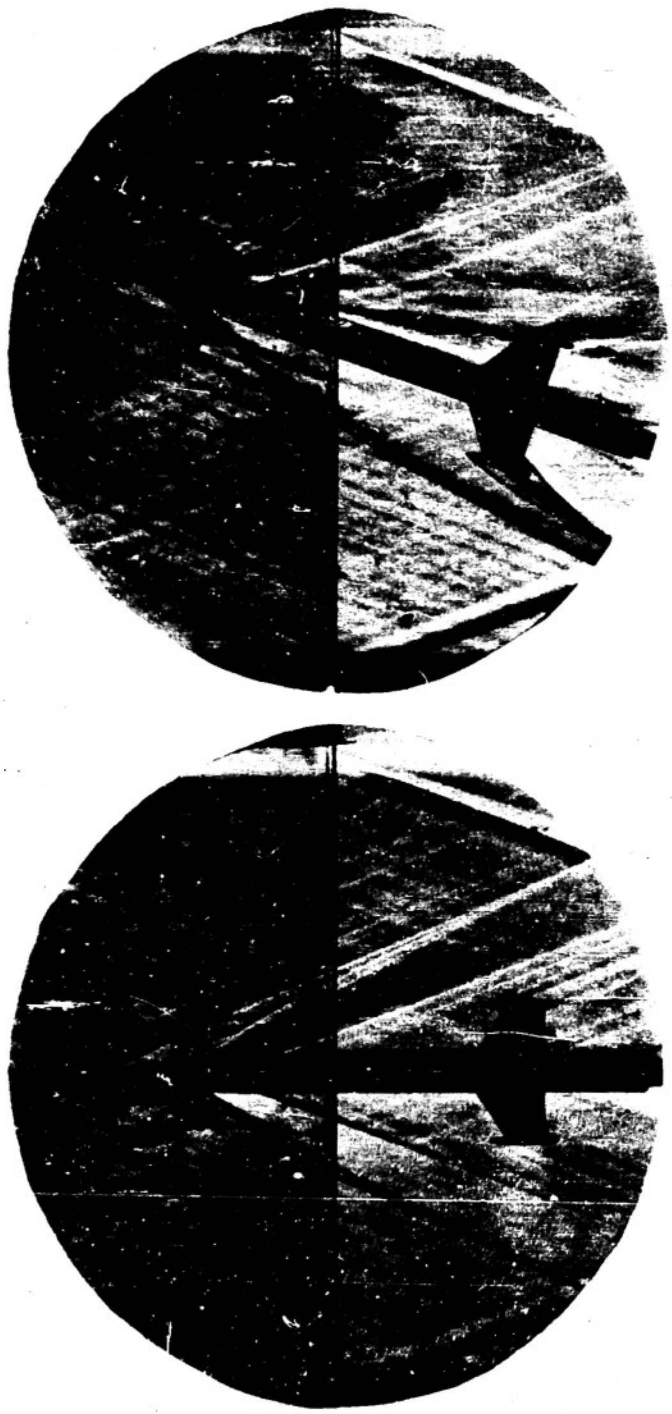

Figure 38

Aeroballistic Research Department
External Distribution List for Applied Math. (X3)

No. of Copies	
	Chief, Bureau of Ordnance Department of the Navy Washington 25, D. C.
1	Attn: Rea
1	Attn: Rexe
3	Attn: Re9a
	Chief, Bureau of Aeronautics Department of the Navy Washington 25, D. C.
1	Attn: AER-TD-414
1	Attn: RS-7
	Commander U.S. Naval Ordnance Test Station Inyokern P.O. China Lake, California
2	Attn: Technical Library
1	Attn: Code 5003
	Commander U.S. Naval Air Missile Test Center Point Mugu, California
2	Attn: Technical Library
	Superintendent U.S. Naval Postgraduate School Monterey, California
1	Attn: Librarian
	Commanding Officer and Director David Taylor Model Basin Washington 7, D. C.
1	Attn: Hydrodynamics Laboratory
	Chief of Naval Research Navy Research Section Library of Congress
2	Washington 25, D. C.
	Office of Naval Research Washington 25, D. C.
1	Attn: Code 432
1	Attn: Code 438
1	Attn: Code 463
	Director Naval Research Laboratory Washington 25, D. C.
1	Attn: Code 2021
1	Attn: Code 3800
	Research and Development Board Library Branch Pentagon, 3D1041
1	Washington 25, D. C.
	Chief, AFSWP P.O. Box 2610 Washington, D. C.
1	Attn: Technical Library

No. of Copies	
	Air Targets Division Directorate of Intelligence Headquarters, USAF Washington 25, D. C.
1	Attn: Chief, Physical Vulnerability Br.
1	Attn: AFDRD-RE
	Commanding General Hdqts, Wright Air Development Center Wright-Patterson Air Force Base Dayton, Ohio
1	Attn: WCSO
7	Attn: WCAPD
2	Attn: WCRR
	Physics Branch Division of Research U. S. Atomic Energy Commission
1	Washington 25, D. C.
	Director Maxwell Air Force Base, Alabama
1	Attn: Air University Library
	The Artillery School Antiaircraft and Guided Missiles Br. Fort Bliss, Texas
2	Attn: Research and Analysis Sec.
1	Attn: Pres. Army Field Forces, Board #4
	Ballistic Research Laboratories Aberdeen Proving Ground Aberdeen, Maryland
2	Attn: D.S. Dederick
	National Bureau of Standards Washington 25, D. C.
1	Attn: Nat'l Applied Math. Lab.
1	Attn: W. Ramberg
1	Attn: Librarian(Ord. Dev. Div.)
	National Bureau of Standards Corona Laboratories (Ord. Dev. Div.) Corona, California
1	Attn: Dr. Harold Thomas
	National Bureau of Standards Building 3U, UCLA Campus 405 Hilgard Avenue
1	Los Angeles 24, California
	Attn: Librarian
	University of California Berkeley 4, California
1	Attn: G. J. Maslach
1	Attn: Dr. S.A. Schaaf
	VIA: InsMat
	California Institute of Technology Pasadena 4, California
2	Attn: Librarians(Guggenheim Aero Lab)
1	Attn: Prof. M.S. Plesset
	VIA: BuAero Rep.

No. of Copies	
	University of Illinois 202 E. R. L. Urbana, Illinois
1	Attn: Prof. A.H. Taub VIA: InsMat
	Director Fluid Dynamics and Applied Math. University of Maryland College Park, Maryland
1	VIA: InsMat
	University of Michigan Engineering Research Institute Ypsilanti, Michigan
1	Attn: J.W. Carr, III
	Willow Run Research Center Willow Run Airport University of Michigan Ypsilanti, Michigan
1	Attn: L.R. Biasell VIA: InsMat
	University of Minnesota Rosemount, Minnesota
1	Attn: J. Leonard Frame VIA: Ass't InsMat
	Dept. of Aero. Engr. The Ohio State University Columbus, Ohio
1	Attn: G.L. Von Eschen VIA: Ass't InsMat
	Polytechnic Institute of Brooklyn 99 Livingston Street Brooklyn 2, New York
1	Attn: Dr. Antonio Ferri VIA: ONR
	University of Wisconsin Naval Research Laboratory 422 Farm Place
1	Madison 6, Wisconsin VIA: InsMat
	Princeton University Forrestal Research Center Library Project Squid Princeton, New Jersey
1	Attn: M. H. Smith
	Armour Research Foundation 35 West 33rd Street Chicago 16, Illinois
1	Attn: Engr. Mech. Div.
	Applied Physics Laboratory The Johns Hopkins University 8621 Georgia Avenue Silver Spring, Maryland
1	Attn: Arthur G. Norris VIA: NIO

No. of Copies	
	Defense Research Laboratory University of Texas Box 1, University Station
1	Austin, Texas Attn: InsMat
	Eastman Kodak Company 50 West Main Street Rochester 4, New York
2	Attn: Dr. H. Trotter, Jr. VIA: NIO
	General Electric Company Bldg. #1, Campbell Avenue Plant Schenectady, New York
1	Attn: Joseph C. Hoffman VIA: InsMach.
	The Rand Corporation 1500 Fourth Street Santa Monica, California
1	Attn: Librarian VIA: InsMat
	Douglas Aircraft Company, Inc. 3000 Ocean Park Boulevard Santa Monica, California
1	Attn: E.F. Burton VIA: BuAero Rep.
	North American Aviation, Inc. 12214 Lakewood Boulevard Downey, California
2	Attn: Aerophysics Library VIA: BuAero Rep.
	National Advisory Committee for Aero 1724 F Street Northwest Washington 25, D. C.
5	Attn: E.B. Jackson
	Ames Aeronautical Laboratory Moffett Field, California
2	Attn: Dr. A. C. Charter
	Langley Aeronautical Laboratory Langley Field, Virginia
1	Attn: Theoretical Aerodynamics Div.
1	Attn: Dr. A. Busemann
1	Attn: J. Stack
	NACA Lewis Flight Propulsion Lab. Cleveland Hopkins Airport Cleveland, 11, Ohio
1	Attn: Dr. John C. Evvard
	Harvard University 21 Vanserg Building Cambridge 38, Massachusetts
1	Attn: Prof. G. Birkhoff
	Johns Hopkins University Charles and 34th Streets Baltimore 18, Maryland
1	Attn: Dr. F. H. Clauser

No. of Copies	
	New York University 45 Fourth Avenue New York 3, New York
1	Attn: Dr. R. Courant
	California Institute of Technology Pasadena 4, Calif.
1	Attn: Dr. Hans W. Liepmann
	University of Toronto Institute of Aerophysics Toronto 5, Ontario
1	Attn: Dr. G. N. Patterson VIA: BuOrd (Ad3)
	Hughes Aircraft Company Missile Aerodynamics Department Culver City, California
1	Attn: Dr. Allen E. Puckett
	Institute for Advanced Study Professor John von Neumann
1	Princeton, New Jersey
	University of Michigan Willow Run Research Center
1	Ypsilanti, Michigan